Medical Image Analysis 54 (2019) 149–167

Contents lists available at ScienceDirect

Medical Image Analysis

journal homepage: www.elsevier.com/locate/media

Ultrasound guidance in minimally invasive robotic procedures☆

Maria Antico[a,b], Fumio Sasazawa[a,b,c], Liao Wu[a,b], Anjali Jaiprakash[a,b], Jonathan Roberts[a,b], Ross Crawford[a,b,d], Ajay K. Pandey[a,b], Davide Fontanarosa[b,e,f,*]

[a] School of Chemistry, Physics and Mechanical Engineering, Queensland University of Technology (QUT), Brisbane, Queensland, Australia
[b] Institute of Health & Biomedical Innovation, Queensland University of Technology, Brisbane, Queensland, Australia
[c] Department of Orthopaedic Surgery, Hokkaido University Graduate School of Medicine, Sapporo, Japan
[d] Department of Orthopaedic Surgery, Prince Charles Hospital, Chermside, Queensland, Australia
[e] School of Clinical Sciences, Queensland University of Technology, Brisbane, Queensland, Australia
[f] Department of Radiation Oncology (MAASTRO), GROW – School for Oncology and Developmental Biology, Maastricht, the Netherlands

ARTICLE INFO

Article history:
Received 30 November 2017
Revised 1 January 2019
Accepted 9 January 2019
Available online 11 January 2019

Keywords:
Ultrasound
Minimally invasive
Robotic
Surgery

ABSTRACT

In the past decade, medical robotics has gained significant traction within the surgical field. While the introduction of fully autonomous robotic systems for surgical procedures still remains a challenge, robotic assisted interventions have become increasingly more interesting for the scientific and clinical community. This happens especially when difficulties associated with complex surgical manoeuvres under reduced field of view are involved, as encountered in minimally invasive surgeries. Various imaging modalities can be used to support these procedures, by re-creating a virtual, enhanced view of the intervention site. Among them, ultrasound imaging showed several advantages, such as cost effectiveness, non-invasiveness and real-time volumetric imaging. In this review we comprehensively report about the interventional applications where ultrasound imaging has been used to provide guidance for the intervention tools, allowing the surgeon to visualize intra-operatively the soft tissue configuration in real-time and to compensate for possible anatomical changes. Future directions are also discussed, in particular how the recent developments in 3D/4D ultrasound imaging and the introduction of advanced imaging capabilities (such as elastography) in commercially available systems may fulfil the unmet needs towards fully autonomous robotic interventions.

1. Introduction

Minimally invasive surgery (MIS) is usually associated with a long learning curve due to technical limitations faced by surgeons in dealing with limited field of view and complete lack of depth perception (Vitiello et al., 2013; Elgezua et al., 2013). Introduction of robotic technology to MIS has been proposed to bring accuracy and precision and the early clinical adoption of robots in surgery dates back to 1980s. By 1994 voice controlled camera holding robots were demonstrated to work in symbiosis with surgeons performing complex laparoscopic surgery (Sackier & Wang, 1994). The major breakthrough came in early 1997 when Intuitive Surgical introduced a multi arm robot named da Vinci that became very helpful in enhancing dexterity and manoeuvrability. Since then developments of robotic systems in clinical applications has led to innovative changes in medical procedures and demand for minimally invasive healthcare (Leven et al., 2005; Elgezua et al., 2013) has significantly increased. Compared to the purely mechanical and manually manipulated instruments, the robotic instruments have better manoeuvrability, as more degrees of freedom can be actuated simultaneously than what could be directly handled by human hands. They are also more intelligent since more sensors can be integrated and processed during the operation to monitor the process and assist in decision making (Wu et al., 2018). Medical robots are now equipped with imaging systems that can create an enhanced view of the interventional site and real-time

Abbreviations: 2D/3D/4D, 2/3/4 Dimensional; BPH, Benign Prostate Hypertrophy; CEUS, Contrast-Enhanced Ultrasound; CPB, Cardiopulmonary Bypass; CPU, Central Processing Unit; EM, Electromagnetic; FOV, Field of view; GPU, Graphics Processing Unit; HCC, Hepatocellular Carcinoma; HT, Hough Transform; ICP, Iterative Closest Point Algorithm; LLS, Left Lateral Sectionectomy; MIS, Minimally Invasive Surgery; MRI, Magnetic Resonance Imaging; MW, Microwave; NVB, Neurovascular Bundle; PNET, Pancreatic Neuroendocrine Tumor; RALRP, Robotic-Assisted Laparoscopic Radical Prostatectomy; RANSAC, Random Simple Consensus; RF, Radio Frequency; SAA, Splenic Artery Aneurysms; SURF, Speeded Up Robust Features; TEE, Transesophageal Echocardiography; TPS, Treatment Planning System; TRUS, Transrectal Ultrasound; TRUSE, Transrectal Ultrasound Elastography; US, Ultrasound; LUS, Laparoscopic Ultrasound; USE, Ultrasound Elastography.

☆ Conflicts of interest: No actual or potential conflicts of interest exist.

* Corresponding author at: Gardens Point Campus, 2 George St, Brisbane, Queensland 4000, Australia.
E-mail address: davide.fontanarosa@maastro.nl (D. Fontanarosa).

https://doi.org/10.1016/j.media.2019.01.002
1361-8415/

navigation tracking of surgical tools for effective synchronization with pre-operative plans has now become reality (Lee et al., 2010; Leven et al., 2005; Ho et al., 2011). MIS patients now benefit from faster recovery times owing to small incisions required to access the area of surgical interest and development of patient specific digital models. In orthopaedics, medical robotic platforms such as MAKO (Stryker, Kalamazoo, Michigan, U.S.A.) has proven to be very successful in knee and hip arthroplasty where registration of rigid-bones with robotic tools has resulted in better patient outcomes (van der List, Chawla, & Pearle, 2016). On the other hand, the use of the Cyberknife System (Accuray, Sunnyvale, CA, USA) has proven to be equally beneficial in dealing with patient specific radiation therapy outcomes (Wang et al., 2015). Recently, researchers from the University of Oxford have completed the first successful trail of robot-assisted retinal surgery using PRECEYES Surgical System (Edwards et al., 2018). However, further development of the robotic-assistant technology is required before medical robots can overcome some of the challenging aspects in dealing with soft tissue deformation and real time volumetric representations required for MIS. There is an apparent lack of volumetric imaging technology that would assign real time situational awareness to medical robots. One of the most common imaging modalities for these applications is ultrasound imaging (US), employed either as sole image-guidance or in combination with other imaging modalities, such as magnetic resonance imaging (MRI) or 2D laparoscopic cameras (Ukimura et al., 2015; Azizian et al., 2014). The major advantages of US are that is cost-effective, non-invasive, and allows real-time volumetric imaging, making it particularly useful for applications where the anatomical structures could move and/or deform during the intervention due to contact with tools or physiological factors (Fenster and Downey, 2001). Advanced US modalities such as colour-Doppler and shear-wave elastography can potentially be used as an additional source of information to differentiate tissues (Schneider et al., 2011; Deshmukh et al., 2014) or to track tools inside the patients' anatomy (Adebar and Okamura, 2013; Schneider et al., 2011).

In this work, we start with reviewing the developments in US-guided robotic procedures linked to MIS in the last decade (2007–2017) and then make the case of how increased adoption of US as a stand-alone or secondary imaging modality would benefit Medical Robotics. For a comprehensive discussion we performed a systematic search in Pubmed including original research articles, clinical trials, experimental studies, reviews and conference proceedings. The search was conducted by combining the keywords "ultrasound", "guidance", "computer-assisted" or "robotic", "minimally invasive" and "procedure" or "surgery" or "intervention" (including Mesh terms automatically provided by PubMed). The search was then further expanded using the relevant references found in the publications obtained with the aforementioned inclusion criteria. We also highlight the existing literature in this area where authors have already reviewed use of robotic US for some specific medical applications (for example (Kaye, Stoianovici, 2014)and (Mahmoud, Aslam, Alsaadi, Fagiri, & Alonazi, 2018)) or proposed general overviews of the use of US in medical robotic procedures (Priester, Natarajan, & Culjat, 2013).To the best of our knowledge there is no comprehensive and specific review on the use of US to guide robotic procedures in MIS, including all the image processing techniques (for example segmentation and tracking).

For a focused presentation, the review is divided into two main parts: robotic percutaneous needle procedures (Section 2) and robotic-assisted minimally invasive surgery (Section 3). The first category includes interventions such as biopsy, brachytherapy, percutaneous ablation and anaesthetic injections. The second category consists of laparoscopy and minimally invasive cardiac surgery. The use of US to detect and track interventional tools is reported in Section 4. Further advancements in medical robots, such as robotic autonomous systems, and the recent developments of 3D/4D US in clinical practice will be reviewed and discussed in Section 5.

2. US-guided robotic percutaneous needle procedures

2.1. Breast and prostate biopsy

Minimally invasive techniques such as US-guided needle biopsies are currently considered standard diagnostic techniques for breast and prostate cancer (Presti, 2008; Newell and Mahoney, 2014). Robotic systems for these types of applications are particularly advisable because of the specific requirements for manual dexterity and precision in "suspicious" tissue identification and extraction, especially in case of small lesions (e.g. small breast lesions with diameters in the range 2–8 mm) (Hruskaa and O'Connor, 2008; Nelson et al., 2012). The possible motion and deformation of prostate and breast during biopsy make the procedure even more challenging. Due to US probe pressure (Baumann et al., 2007), tissue deformations induced by needle insertion (Mallapragada et al., 2007; Mallapragada et al., 2008; DiMaio and Salcudean, 2003) or physiological factors (Chopra et al., 2006; Padhani et al., 1999), the target region might move from the original location. Breast lesions can shift up to 1 cm from the original position due to needle insertion deforming the surrounding tissues (Mallapragada et al., 2008). For the prostate, needle-induced deformation and motion (De Silva et al., 2011; Lagerburg et al., 2005; Stone et al., 2002) is estimated to be as large as 1.5 cm; and physiological factors such as peristaltic motion and bladder filling may generate drifts larger than 1 cm (Padhani et al., 1999; Ghilezan et al., 2005). In these cases, real-time tracking and/or immobilization of the structure of interest are crucial for the success of the operation (Mallapragada et al., 2007). Even though in a standard biopsy the surgeon can typically correct the needle path in real-time when such shifts occur, it may be challenging to re-centre the target and a new insertion could be needed (Mallapragada et al., 2008; Ho et al., 2009), possibly causing unintended collateral morbidities. The introduction of a robotic system can reduce invasiveness, operator dependence and duration of the biopsy (Nelson et al., 2012; Mallapragada et al., 2008).

In the last decade, many US guided robotic systems for breast and prostate biopsy have been developed, mostly at an experimental level (Table 1). The systems designed for this type of procedure are either autonomous or imply a minimum input action from the surgeon (semi-autonomous systems). Typically, in these workflows, a US probe attached to a robotic arm scans the area of interest. The system, or the surgeon, then identifies the target in the US image and the target coordinates are translated to another robotic arm holding the needle, in order to guide it to the insertion point (Fig. 1). The insertion is then either performed by direct actuation of the robotic arm for autonomous systems or controlled by the surgeon in semi-autonomous cases.

2.1.1. Autonomous systems

An autonomous robotic system compensating for intra-operative target motion was designed by Mallapragada et al. and tested on a breast phantom (Mallapragada et al., 2007; Mallapragada et al., 2008; Mallapragada et al., 2009). The system made use of image processing algorithms to identify and localize the target within the phantom. They also implemented a manipulation device consisting of a set of actuators, which could apply an external force on the phantom surface in case of misalignment with the needle path, thus allowing real-time alignment with the needle trajectory during insertion. Liang et al. (2011) addressed in a more realistic way the target identification and localization tasks proposing a new design of a robotic needle insertion system. In their work they tested a threshold algorithm (plus post processing

Table 1
US-guided robotic percutaneous needle applications.

	Study & year	Robotic system	Study type (CL/FS)[A]	Anatomy Identification	Limitations[B]	Tool Identification	Tracking system	Probe type
Breast biopsy	Mallapragada et al. (2007, 2008, 2009)	Autonomous	FS (phantom)	Search algorithm to localize target in the volume & image processing to determine its coordinates	Details about search algorithm NS & simulation on phantom	Needle position with respect to the image is coded in the controller	Potentiometer for probe localization	2D US
	Liang et al. (2011)	Autonomous	FS (turkey breast)	Threshold algorithm & post processing imaging to segment the breast calcification & cyst	Not sophisticated algorithm plus specific only for calcification and cyst, no motion management	Needle position controlled by the robotic frame	Probe in a fixed known position with respect to the robot frame and needle tip	3D US
	Nelson et al. (2012)	Semi-autonomous	FS (phantom)	High image quality obtained through a developed scanner	Target contoured by physician, no motion management	Needle localization through sensor on robotic arm	Probe localization through sensor on robotic arm	NS[C]
Prostate biopsy & Brachytherapy	Bassan et al. (2007)	Semi-autonomous	FS (phantom)	3D US image reconstructed by automatic probe holder rotation, point of interest marked by clinician	Target contoured by physician, no motion management	Needle localization through sensors on robotic arm	Probe localization through sensors on robotic arm	2D TRUS
	Yu et al. (2007)	Autonomous/ Semi-autonomous mode	FS (phantom)	3D US image reconstructed by automatic probe holder rotation, Manual segmentation of anatomical structures of interest	Target superimposed to 3D model to highlight target shift to facilitate the surgeon in needle path correction, but no organ tracking	TPS integrating seeds and needle position; Seeds segmentation NS	Probe localization through sensors on robotic arm	2D TRUS
	Fichtinger et al. (2008)	Autonomous/ Semi-autonomous mode	FS (phantom) & CL ($n=5$)	3D US image reconstructed by manual probe holder translation; Manual segmentation of anatomical structure of interest & automatic model creation of the prostate; US probe moved manually to image the plane of the tool tip	Target motion visualized by superimposition of TRUS live images on pre-op 3D model, but no organ tracking	TPS integrating seeds and needle position (localized with optical tracking); Seeds segmentation performed by knowing expected location	Probe localization through sensors on robotic arm	2D TRUS
	Kaicheng et al. (2010)	Autonomous	FS (turkey breast)	Threshold algorithm for surface reconstruction to center probe field of view & calculate depth for tissue extraction	Poor segmentation algorithm, no organ tracking	Needle fixed to probe	Probe localization through sensors on robotic arm	3D US
	Ho et al. (2011)	Semi-autonomous	CL ($n=20$)	3D US image reconstructed by automatic probe holder translation along cranio-caudal direction, Manual segmentation of the prostate & automatic model creation	No tracking of anatomical structure	Needle localization through sensors on robotic arm	Probe localization through sensors on robotic arm	2D TRUS
	Hungr et al. (2009), Long et al., (2012)	Autonomous	FS (phantoms)	Manual segmentation and tracking of prostate using image registration	Phantom study considering only the prostate	Needle localization through sensors on robotic arm	Probe localization through sensors on robotic arm	3D TRUS

(*continued on next page*)

Table 1 (*continued*)

	Study & year	Robotic system	Study type (CL/FS)[A]	Anatomy Identification	Limitations[B]	Tool Identification	Tracking system	Probe type
	Zhang et al. (2016)	Semi-autonomous	FS (phantom &5 patient images)	MRI-TRUS fusion and automatic target detection using elastic registration, US probe moved automatically to image the plane of the tool tip	Simulations performed on static patient images	EM tracking for needle localization	EM tracking for probe localization	2D TRUS
Lung Brachytherapy	Trejos et al. (2007) (2007) & Lin et al., (2008)	Tele-operation	FS (surgical box containing a lung phantom)	Navigation system allows to see 2D plane of interest	Target contoured by physician, no motion management	Ultrasound image information and EM tracking to recreate the needle image in the navigation system	EM tracking for probe localization	2D US
Anaesthesia for saphenous nerve	Hemmerling et al. (2013)	Tele-operation	CL ($n = 13$)	Interface showing external video and US image, target identified by visual inspection	Only visual inspection for structure and needle recognition	Visual inspection	Probe manually held & no tracking (robot motion operated by surgeon based on direct vision and camera vision)	2D US
Anaesthesia for facet joint	Esteban et al. (Esteban et al., 2018)	Semi-autonomous	CL ($n = 2$)	3D US volume acquired with automatic 2D sweep of probe, needle entry and final points manually selected from physician	Target selected by visual inspection	Needle fixed to probe	Probe localization through sensors on robotic arm	2D US
Liver ablation	Boctor et al.(Emad M. Boctor, Michael A. Choti, 2008)	Semi-autonomous	FS (bovine liver, live porcine model)	3D US image reconstructed from 2D images, semi-automatic segmentation of tumour and vessels, registration with intra-operative images	No real -time motion management, and registration computation time NS	EM tracking or sensors on robotic arm for needle localization	EM tracking for probe localization	2D US
	Xu et al.(2010)	Semi-autonomous	FS (artificial phantom, bovine liver)	3D US image reconstructed from 2D images, visual inspection to select target	Target visually identified by surgeon, no motion management	EM tracking or sensors on robotic arm for needle localization	EM tracking for probe localization	2D US
Prostate ablation	Faber et al.(2015)	Semi-autonomous	FS (canine model)	Prostate individuated in 2 perpendicular planes simultaneously	Target contours selected by physician	Probe localization through sensors on robotic arm	NS	TRUS

Inclusion criteria: In the referenced studies ultrasound is used to guide robotic surgery at a clinical or feasibility study.

[A] FS = Feasibility study; CL = Clinical study.

[B] The limitations specified are only related to the identification, visualization and tracking the anatomy.

[C] NS = Not specified.

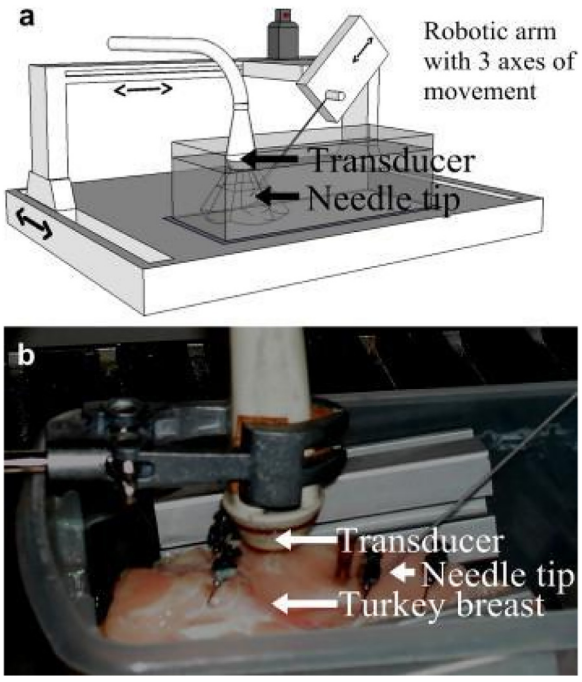

Fig. 1. An example of robotic system, composed by: a robotic arm holding the needle for the intervention and a robotic US probe holder with the transducer fixed at his end. The robotic components are shown schematically (a) and during an experimental study on animal model (b) (Liang et al., 2011).

to eliminate noise and artefacts) for cyst and calcification identification on turkey breast (Whitman et al., 2007). Despite more elaborate segmentation algorithms having been proposed in literature (Boukerroui et al., 2001; Horsch et al., 2002), a less sophisticated algorithm has been selected in this study to reduce computation time. For the system proposed by Nelson et al. (2012) motion management was not specified.

For applications in prostate biopsy image guidance is performed using transrectal ultrasound (TRUS). Tumor masses within the prostate are usually not visible with this imaging modality (Sonn et al., 2014). Therefore a multiple-core biopsy is generally performed (Matlaga et al., 2003) with the aim of collecting uniformly distributed tissue samples from the prostate volume. Although several authors proposed MRI-TRUS fusion (Hadaschik et al., 2011; Sonn et al., 2014; Xu et al., 2008; Ukimura et al., 2015) for prostate lesion detection, due to several factors, such as high costs and extended biopsy duration (Hadaschik et al., 2011), currently 12 core-biopsy represents the "gold standard" for prostate tumor diagnosis (Presti, 2008). Bax et al. (2008) developed a system able to track the TRUS position and to enable needle biopsy planning. Starting from this work, several robotic platforms performing multiple-core biopsies have been proposed in literature. Liang, Rogers, Light, von Allmenb and Smith (2010) simulated a 8-core biopsy on a turkey breast using an autonomous robotic system. The authors developed a threshold algorithm to reconstruct the target surface that was then used to define the locations of the tissues to be sampled. During the simulations, the turkey phantom was fixed with pins to prevent motion and thus no correction mechanism has been developed to account for intra-operative prostate motion. The turkey phantom, though, did not realistically mimic the prostate tissue and the segmentation algorithm implemented resulted in some cases in poor surface reconstruction.

2.1.2. Semi-autonomous systems

For breast biopsy applications a semi-autonomous systems was proposed by Nelson et al. (2012), implementing a high image quality US scanner (Nelson et al., 2007) for lesions identification. In this setup, the breast was scanned through an acrylic container filled with water and coupled with the US probe using US gel. This way, tissue compression due to probe pressure was avoided and the probe field of view was optimized. Before needle insertion, the target and the needle path were selected on a 3D US volume by the clinician using a graphic interface. No target motion management was implemented to correct for possible target shifts.

A semi-autonomous robotic system (BioXbot) (Ho et al., 2009) for prostate biopsy was implemented by Ho et al. (2011) and tested in a clinical pilot study. The prostate was manually segmented from the 2D TRUS images and a 3D model was created. Based on the prostate dimensions and position, the system planned the location of the tissues to be sampled and the needles trajectories. The robotic arm then automatically placed each needle in position to be fired by the surgeon. Prior to needle insertion, the surgeon was also able to check the needle trajectories represented as dots on the real-time TRUS images. Prostate motion could be detected by the surgeon in the graphical interface as a misalignment between the prostate model and the live images, but no automatic tracking was implemented.

2.2. Prostate and lung brachytherapy

Besides biopsy, US-guided robotic applications involving percutaneous needle insertions, with the same configuration of components (as in Fig. 1), have also been developed for brachytherapy and more recently for focal therapy (Nguyen and Jones, 2011) (also referred to as "ablation") (Table 1).

Brachytherapy involves the implantation of radioactive seeds to destroy locally the cancerous cells. Typically a total of 80–100 seeds are implanted in about 20 needle insertions (Ding et al., 2006). Prior to implantation, a treatment planning system (TPS) determines the number of seeds and their position in order to generate the desired dose distribution in the tissues. To achieve correct tumour coverage and minimize toxicity, it is of paramount importance that the seeds are positioned as simulated. Therefore, as for biopsy, motion management is important to ensure a successful intervention.

Brachytherapy is a procedure also used as treatment for lung cancer, commonly for patients not eligible for surgical tumour resection. It plays an important role in endobronchial obstruction removal for palliative patients with bronchus cancer (Skowronek, 2015). As for prostate brachytherapy, this treatment modality presents many challenging aspects that can be mitigated by combining US imaging and robotic systems, among which: accurate needle placement, stable needle retraction and access to the area of interest due to the proximity of bones, vessels and nerves. Moreover, uncertainties in tumour location are generated by heart beating and respiration (Trejos et al., 2007). While a robotic system can improve accuracy and stability during needle placement and retraction, US imaging might be helpful to establish optimal needle insertion points and orientation as well as monitor organ motion during the procedure.

2.2.1. Autonomous systems

Long et al. (2012a) proposed an autonomous system (Prosper) for prostate brachytherapy which could track and compensate for the motion of the prostate in real time during the procedure using 3D US. However, details about the registration algorithm and computation times were not specified and the procedure was only tested on a deformable phantom. Yu et al. (2007) and Fichtinger et al. (2008) proposed instead to monitor prostate motion during needle placement comparing it to a model of the gland generated prior to the intervention from 2D manual contouring.

During intervention, for each seed the optimal position was recalculated based on the ones already placed to compensate for possible shifts or deformations in the prostate.

2.2.2. Semi-autonomous systems

Zhang et al. (2016) developed a semi-autonomous robotic system for prostate brachytherapy implementing an MRI-TRUS automatic deformable registration platform. The brachytherapy plan was created on a preoperative fusion between the two modalities, and needle insertion was performed navigating on the live TRUS images co-registered to the MRI volume using a maximum correlation coefficient deformable registration method.

Other studies (Bassan et al., 2007; Yousef et al., 2007; Podder et al., 2007) in the area of prostate brachytherapy focussed more on developing sophisticated needle robotic manipulators or probe holders than specifically on intra-operative US guidance. For example, Bassan et al. (2007) developed a complete system integrating a novel robotic manipulator for the seed injector and a probe holder allowing for 3D image reconstruction through rotation of the US probe.

2.2.3. Teleoperated systems

For lung brachytherapy, despite the clinical and scientific need, only one system has been proposed in the past decade in literature, by Trejos et al. (2007). Their solution consisted in two teleoperated surgical robotic systems (ZEUS and AESOP), used to control an endoscope, an US probe, a tool for incision and a seed injector. The surgeon guided the intervention by means of a navigation interface (InterNAV), showing position and orientation of the needle and of the US probe. The needle trajectory was projected onto the US images, together with the target outlined by the surgeon. The system was subsequently modified improving the robotic controller and updating the graphical interface (Lin et al., 2008).

2.3. Liver and prostate ablation

Ablation is a relatively new treatment option for hepatocellular carcinoma (HCC), which covers 85–90% of all primary liver cancers (El-Serag and Rudolph, 2007; Xu et al., 2010) and for endoscopic benign prostatic hyperplasia (BPH) dissection. Ablation consists of destroying cancerous cells by means of chemical injections, cryotherapy or thermal energy produced by radiofrequency, microwave (MW) or focused US (Boctor et al., 2008). Among thermal ablation techniques, percutaneous microwave and radiofrequency ablation are currently considered the most effective to treat early stage HCC (Poulou et al., 2015). During these procedures, a needle-like device (ablation tool) is inserted into the tumour under US guidance and once in position the energy to eradicate the tumour is released (Boctor et al., 2008).

Although the percutaneous access to the tumour limits the invasiveness of the intervention, it increases the complexity of the treatment procedure. In fact, it is often necessary to perform difficult manoeuvres and precise and accurate needle insertion with limited field of view while compensating for possible organ mobility (Xu et al., 2010; Eisele, 2016).

2.3.1. Semi-autonomous systems

Boctor et al. (2008) and Xu et al. (2010) implemented semi-autonomous robotic systems for liver ablation, improving ergonomics, target visualization and guidance. The systems comprised the ablation tool, a robotic arm to guide it to the insertion position, a 2D US probe and a navigation interface. In the workflow introduced, the needle trajectory was planned on a 3D US volume that had been manually scanned using a 2D US probe localized with electromagnetic (EM) tracking (Rohling et al., 1999). During the ablation procedure, the probe was manually held and the live 2D US image could be visualized in the navigation interface with the current position and the planned trajectory of the needle. A schematic representation of the procedure set-up is shown in Fig. 2.

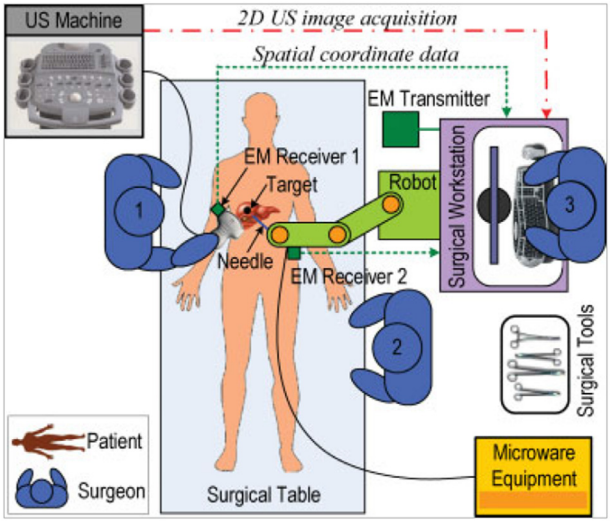

Fig. 2. Schematic representation of the procedure set-up for US-guided ablation robotic system. The robotic arm holding the MW ablation tool is operated form the surgical workstation, where the surgeon through a navigation interface can visualize the live 2D US images. The US probe, EM tracked, is manually guided by an assistant surgeon (Xu et al., 2010).

In the work of Xu et al. (2010), a microwave simulator was also added to the system, in order to plan the microwave power and duration to generate necrosis in the whole tumour volume. To increase precision and safety, Boctor et al. (2008) added a registration procedure to detect tumour position changes. The regions of interest (tumour and vessels) were semi-automatically segmented, using an adaptive-level set algorithm (Xu et al., 2007). In order to confirm intra-operatively that the location of the regions of interest was as simulated, an iterative closest point algorithm (ICP) was used to deform the vessels in the intra-operative images to the corresponding structures in the pre-operative image (Rusinkiewicz and Levoy, 2001; Besl and Neil D. McKay, 1992). In case of tumour location change, the patient was asked to regulate breathing to restore the original tumour position (Sabo et al., 1999). The registration procedure was performed upon request by the surgeon. Details about registration computation time were not specified.

For prostate cancer, Faber et al. (2015), instead, developed and tested on a canine model a novel robotic device for managing symptomatic BPH with hydrodissection ablation, that uses a high velocity saline stream for tumor resection. Prior to the ablation procedure, the device (PROSPECT Aquablation™ system, PROSPECT BioRobotics, Redwood Shores, CA) scanned the prostate gland with a TRUS probe (Model 8848; B and K Medical, Denmark) and computes an ablation plan, based on the US images acquired. The surgeon can then adjust the settings pre-computed by the system. The console can be used to precisely regulate the fluid pressure, the transducer motion and the laser output for cauterization after the ablation phase.

2.4. Anaesthetic injections

US-guided nerve block is typically carried out by identifying the saphenous nerve from US images followed by an anaesthetic injection. The injection can be performed at the ankle, knee or malleolus level, and it is generally used for postoperative analgesia (Varitimidis et al., 2009). Recently, an US-guided robotic sys-

tem has also been implemented for facet joint injections, to provide back and spinal pain relief (Esteban et al., 2018).

2.4.1. Semi-autonomous systems

Esteban et al. (2018) implemented a robotic system, involving a semi-autonomous US scan to reconstruct the ROI volume, by automatically sweeping a 2D US probe between two points selected by the surgeon. The US probe and the needle holder were fixed to the end effector of a robotic arm. The acquired US volume was used to plan the needle insertion. The physician selected the needle entry and final point and the system computed the optimal needle path and guided the needle to the initial position, with the planned needle inclination.

2.4.2. Teleoperated systems

In order to guarantee stable incision and faster learning curve, Hemmerling et al. (2013) and Morse et al. (2014) developed a robotic system (Magellan) in which the needle was held and guided by a robotic arm, remotely controlled by a joystick. To select the point for needle insertion, the combined information from a camera and from a manually operated 2D US system was visualized and used by the surgeon.

3. US guidance in robotic-assisted minimally invasive surgery (MIS)

3.1. Teleoperated systems for laparoscopy

Surgeons have used US to observe intraperitoneal, retroperitoneal and pelvic organs not only pre- and post- but also during the surgery. In traditional open abdominal surgeries, the surgeons can see organs directly with their eyes, can palpate organs directly with their fingers and, in addition, can put US probes directly on the organs. Using the combination of all these sources of information, they can detect foci of disease to treat (Makuuchi et al., 1998). Since the German gynaecologist Kurt Semm performed the first laparoscopic appendix removal, though, the advancement in this type of surgery has been so remarkable that various laparoscopic procedures became preferable to open approaches (Antoniou et al., 2015). Laparoscopy produces smaller surgical wounds, which brings patients reduced postoperative pain, lower risk of wound infection, and shorter hospital stay (Schols et al., 2013). On the other hand, smaller wounds increase the difficulty for surgeons to palpate organs and to position the US transducer directly on the organs as in open surgeries. To reduce the impact of these disadvantages, intracorporeal laparoscopic US (LUS) was developed and widely accepted among surgeons (Makuuchi et al., 1998). After the introduction of robotically assisted methods, such as the da Vinci robotic system (Intuitive Surgical, Sunnyvale, California) (Fig. 3), several works in literature reported about the combination of the latter with US guidance (Dwyer et al., 2018).

Patriti et al. (2009) used intraoperative US on seven cases of colorectal cancer with synchronous liver metastasis to define liver vascular anatomy and the sites of metastasis, as well as to guide radiofrequency ablation. Calin et al. (2016) focused on a synchronous liver metastasis case, but with pancreatic neuroendocrine tumor (PNET) as primary (Hill et al., 2009). These procedures consist in identifying the vessels in the liver, the boundaries of pancreatic mass to determine the transection line, and the splenic vessels with intraoperative Doppler US. The same imaging modality was adopted by Araujo et al. (2017) to detect hypervascular lesions during robotic laparoscopic liver resection (left lateral sectionectomy (LLS)) (Clavien, 2016) on two cirrhotic patients (Nota et al., 2016). Liu et al. (2015) employed a diagnostic US machine to seek intraoperatively for previously undetected lesions and to determine

Fig. 3. The Da Vinci robotic system (Antoniou et al., 2015).

the accurate surgical resection margins on seven cases of spleen-preserved distal pancreatectomy. Giulianotti et al. (2011) reported on nine splenic artery aneurysms (SAA) cases for whom special made vascular micro-clamps were introduced into the aneurysms by robotically assisted laparoscopic surgery. After the procedure, blood flow was assessed with intraoperative Doppler US.

In all the previously reported cases, the operator had to interact with the robotic and the US components separately (Woo et al., 2014). But the integration of the two systems in a single navigation platform has been the subject of several studies. Walsh et al. (2013) proposed the TilePro™ multi-input display software (Intuitive Surgical, Sunnyvale, California) to integrate real-time 2D transvaginal US and the operative FOV into a single display, in a clinical case of abdominal cerclage placement, a procedure aiming at surgically closing the cervix during pregnancy. Yang et al. (2014) created a navigation system for fetoscopic MIS showing 2D fetoscopic images superimposed on a 3D model of the placenta surface created using 3D US. US was also used as a tracking system for the endoscope, and no external tracking systems, such as optical tracking or EM tracking, were necessary. While the integration in Walsh et al. and Yang et al. was mainly achieved visually, Schneider et al. (2012a) proposed a physical integration of the systems. A 2D linear LUS transducer (Gore Tetrad, Englewood, CO) robotically manipulated with the EndoWrist™ (Intuitive Surgical, Sunnyvale, California) instrument was inserted into the abdominal cavity to scan the liver. US images were then displayed on the stereo display of the robotic surgical console. The superior performance of this integrated system, compared to conventional handheld intraoperative LUS, was demonstrated by tests on phantom livers.

To compensate for the lack of haptic feedback, or palpation, that is a fundamental intraoperative source of information for surgeons in open abdominal surgeries, US elastography (USE) has been used to provide tissue stiffness values to the surgeons (Ophir et al., 1999). Several researchers reported their attempts to adopt USE for this purpose. Schneider et al. (2012b) used a robotically manipulated custom designed 2D US probe (frequency range 7–10 MHz) to create a 3D elastographic map of the surgical site. The probe was positioned on the organ to map and localized mechanically by the robotic system. Shear waves were created in the organ by an external mechanical exciter (LDS Model V203, B&K, Denmark) driven by a signal generator (Agilent 33220A), captured by the probe as radio frequency (RF) data and then processed to generate a 2D elastogram. 3D full volume elastograms were finally reconstructed from the 2D spatially tracked images. The authors demonstrated the accuracy of the system in a phantom model and the feasibility in an *in vivo* setting (Schneider et al., 2012a). Billings et al. (2012) equipped one arm of a robotically assisted MIS

Fig. 4. Two lesions with different stiffness values shown on B-Mode (left top figure) and elastography (left bottom figure) images. On the right, the US probe held by one of the da Vinci robot arms and coupling gel (Billings et al., 2012).

system with a linear array US transducer (Gore, Newark, DE, USA). A non-clinical experimental "palpate controller" interface was installed onto the system to make the robot generate a sinusoidal precise and consistent tissue compression. The US wave reflected from the deformed tissue was captured by the transducer as RF data and processed with graphics processing unit (GPU)-based USE system. The authors evaluated this system with an elasticity phantom model that contains two lesions of different known hardness. While B-mode image showed no difference between the two lesions, USE clearly showed the difference in stiffness (Fig. 4).

Incremental to this work, Deshmukh et al. (2014) introduced real-time US probe external localization using an EM tracking device to provide intraoperative real-time elastographic information to the surgeons. A summary of the here mentioned procedures is reported in Table 2.

3.2. Laparoscopic procedures in urology

3.2.1. Teleoperated systems for prostatectomy

Robotic–assisted laparoscopic radical prostatectomy (RALRP) is a common surgical procedure, accounting for around 70% of the prostate discectomies performed in the United States (Sharma et al., 2009). Several solutions combining the standard laparoscopic camera of the Da Vinci system with real-time TRUS have been proposed, aiming at reducing resection margins (Table 2). Mohareri et al. (2014) proposed (and tested in a canine study and a clinical trial with 20 patients) a sagittal/transverse biplane TRUS transducer (Analogic Corporation, 8 Centennial Drive, Peabody, MA 01960) with a robotic probe holder based on a brachytherapy stepper (CIVCO Medical Solutions, Coralville, IO). The system automatically tracked the tip of the da Vinci surgical instrument by rotating the transducer (Fig. 5).

Han et al. developed a robotic TRUS probe manipulator (TRUS robot), manually controlled by the surgeon with a joystick, combined with a 3D reconstruction/navigation software (Han et al., 2012). The three major components of the TRUS robot were: a passive arm component attached to the operating table; a robotic orientation Remote Centre of Motion (RCM) module, to control the US probe angulation; and a driver module to rotate the US probe around its axis. Once positioned, the 2D TRUS probe (EUP-U533; HITACHI-Aloka Medical, Twins-burg, OH, USA) could scan the entire prostate by rotating about its axis. The gathered images were then segmented and a 3D US volume of the whole prostate gland was reconstructed. A further development advancement was introduced in the system by Stoianovici et al. (2014).The robotic platform, allowing for rotation and translation of the probe along its axis, was tested on 46 RALRP clinical cases. . A similar concept was followed by Long et al. (2012b) who modified the ViKY endoscope manipulator (EndoControl, Dover, DE) to hold a TRUS transducer (8818 Triplane side-fire transducer; BK Medical, Denmark). Five cases were reported where the whole prostate gland was scanned, the tip of the laparoscopic surgical instrument was identified and the location of the neurovascular bundles (NVBs) was confirmed with colour Doppler. Hung et al. (2012) also used the ViKY system with a custom-made TRUS holder, a foot pedal controller and a biplane TRUS probe (Type 8818 biplane TRUS probe; B-K Medical, Copenhagen, Denmark). The resulting system was used on 10 prostate cancer patients.

While some reports had already been published about transrectal USE (TRUSE) for prostate biopsy (König et al., 2005; Sumura et al., 2007), Fleming et al. (2012) evaluated this imaging modality as a palpation equivalent tool in robotically assisted MIS. USE was compared with 1) manual palpation and 2) MRI and pathology. In the study 1), synthetic phantoms made from Liquid Plastic (M-F Manufacturing Co., Inc., Haltom City, TX) and ex-vivo phantoms constructed from raw chicken breast were palpated by 25 recruited local students. Then the same phantoms were scanned by the USE and the tumour detection rates were compared. The prototype laparoscopic US probe for robotic system was made with Gore Tetrad's transducer (Gore Tetrad, Englewood, CO) and a US scanner (Analogic Corporation, 8 Centennial Drive, Peabody, MA 01960). USE showed higher sensitivity and specificity (84%, 71%) than those of manual palpation (66%, 67%). Especially in cases with the tumours located deeper than 20 mm, USE showed 66% of detection whereas manual palpation showed 0%. In the study 2), ex-vivo prostate specimen excised from patients were scanned with a Siemens VF 10–5 linear array and a Siemens Antares US scanner (Siemens Medical Solutions USA, Inc. Ultrasound Division, Issaquah, WA) to evaluate the tumour properties and compare with MR imaging and pathological results. USE was proved to have possibility to identify the properties of tumours such as hard or soft, malignant or benign, and central or peripheral (Fleming et al., 2012).

3.2.2. Teleoperated systems for partial nephrectomy & adrenalectomy

Partial nephrectomy and partial adrenalectomy refer to the surgical removal of tumour in kidneys and in adrenal glands respectively. Currently, laparoscopic surgery is considered the gold standard for benign adrenal tumours (Kumar et al., 2009) and for small to medium sized kidney tumours (less than 7 cm) (Nadler et al., 2009). Many benefits can be associated with the introduction of robotics in this type of surgery, such as enhanced dexterity and fine movements control, enhanced magnification and shorter operating time (Kumar et al., 2009; Aboumarzouk et al., 2012) (Table 2). Surgical ablation (Izquierdo-Luna et al., 2016) or a combination of surgery and ablation (usually for tumoural masses smaller than 5 cm) has also been proposed (Nadler et al., 2009).

Robotic-assisted partial nephrectomy (Cabello et al., 2009; Gill et al., 2011; Yakoubi et al., 2012; Papalia et al., 2012; Kaczmarek et al., 2013; Bhayani and Snow, 2008; Rogers et al., 2009) or adrenalectomy (Kumar et al., 2009; Asher et al., 2011) are performed using three or more laparoscopic or robotic ports. Generally, one port is reserved for a camera. Two other openings are used for the robotic trocars, typically guided from the console by the surgeon. Extra ports may be used in case additional tools are needed such as, for example, a LUS probe (Yakoubi et al., 2012), used to identify intra-operatively the tumour and its margins. From the console, the surgeon can see both the camera view and the real-time US images from the laparoscopic probe, in two separate interfaces. . For partial nephrectomy several studies proposed augmented reality imaging systems, fusing the camera and the LUS view. By localizing the anatomy viewed in the US images, it is possible to overlay the image with the laparoscope view. This en-

Table 2
US-guided robotic MIS.

	Study & year	Study type (CL/FS)[A]	Anatomy Identification	Tool tracking	Tracking system for probe	Probe type
Laparoscopy	Patriti et al. (2009)	CL ($n=7$)	Visual inspection	Probe localization through sensors on robotic arm	–	2D LUS
	Giulianotti et al. (2011)	CL ($n=9$)	US Doppler to assess blood flow	Probe localization through sensors on robotic arm	–	NS
	Schneider et al. (2012a)	FS (phantom livers)	US Doppler and B mode for vessel localization and registration with CT	Probe localization through sensors on robotic arm	EM tracking	2D LUS
	Schneider et al. (2012b)	FS (phantom and *in vivo*)	3D reconstructed USE map	–	Probe localization through sensors on robotic arm	2D US
	Billings et al. (2012)	FS (phantom)	USE to differentiate tissue hardness not identifiable from B mode images	Probe localization through sensors on robotic arm	–	LUS
	Walsh et al. (2013)	CL ($n=1$)	US and camera view integrated in single display for abdominal cerclage placement	Probe localization through sensors on robotic arm	–	2D transvaginal US
	Deshmukh et al. (2014)	FS (phantom and *in vivo* pig)	USE with probe localization	Probe localization through sensors on robotic arm	EM tracking	LUS
	Yang et al. (2014)	FS (phantom)	2D images displayed within a US-based 3D placenta surface	Probe localization through sensors on robotic arm	–	3D US
	Liu et al. (2015)	CL ($n=7$)	Visual inspection for lesions and tumoural margins in the pancreas	Probe localization through sensors on robotic arm	–	LUS
	Calin et al. (2016)	CL ($n=1$)	US Doppler to visualize pancreas and liver vessels	Probe localization through sensors on robotic arm	–	NS
	Araujo et al. (2017)		US Doppler to visualize hypervascular lesions in the liver			
Prostatectomy	Mohareri et al. (2014)	FS (canine model) CL ($n=20$)	US images were tool tip present shown	Probe localization through sensors on robotic arm	Probe localization through sensors on robotic arm	2D TRUS
	Han et al. (2012)		3D US volume of prostate reconstructed by rotation of 2D TRUS and manual segmentation	Probe localization through sensors on robotic arm	Probe localization through sensors on robotic arm	2D TRUS
	Long et al. (2012b)	CL ($n=5$)	Tool identification and US Doppler to visualize NVBs	Probe localization through sensors on robotic arm	Probe localization through sensors on robotic arm	2D TRUS
	Hung et al. (Hung et al., 2012)	CL ($n=10$)	Intra-operative visualization of prostate	Probe localization through sensors on robotic arm	Probe localization through sensors on robotic arm	TRUS
	Stoianovici et al. (2014)	CL ($n=46$)	B mode and US Doppler to visualize NVBs	Probe localization through sensors on robotic arm	Probe localization through sensors on robotic arm	LUS
Nephrectomy	(Cabello et al., 2009)	NS	Visual inspection for tumour boundary detection, US and camera views separated in two displays	–	Probe localization through sensors on robotic arm	NS
	Yakoubi et al., (2012)	FS (pig model)		Probe localization through sensors on robotic arm	Probe localization through sensors on robotic arm	LUS
	Kaczmarek et al., (2013)	CL ($n=22$)		Probe localization through sensors on robotic arm	Probe localization through sensors on robotic arm	LUS
	Rogers et al. (2009)	CL ($n=22$)		Probe localization through sensors on robotic arm	Probe localization through sensors on robotic arm	LUS
	Bhayani and Snow (2008)	CL ($n=20$)	Visual inspection for tumour boundary detection, US and camera views integrated in one display	Probe localization through sensors on robotic arm	Probe localization through sensors on robotic arm	LUS
	Edgcumbe et al.(Edgcumbe et al., 2015)	FS (phantom)	Fusion of the LUS image with the laparoscope view	Probe localization through sensors on robotic arm	Real-time optical pattern tracking	LUS
	Zhang et al. (Zhang et al., 2017)	FS (phantom and ex-vivo)	Motion estimation from vision system prior to US scan, and used to move the probe intra-operatively, Segmentation of tumour (algorithm NS)	Probe localization through sensors on robotic arm	Real-time optical pattern tracking	LUS
	Singla et al. (Singla et al., 2017)	FS (kidney phantom)	Overlay the LUS image with the laparoscope view	Probe localization through sensors on robotic arm	Real-time optical pattern tracking	LUS
	Schneider et al. (Schneider et al., 2016)	FS (phantom, 5 patients images)	LUS to identify the blood vessels and register the US image to a preoperative CT	Probe localization through sensors on robotic arm	Real-time optical pattern tracking	LUS
	Gill et al. (2011), Papalia et al. (2012)	CL ($n=12$)	Visual inspection for intra-operative tumour boundary detection, US and camera in two separate displays, US Doppler to monitor blood flow	Probe localization through sensors on robotic arm	NS	LUS

(*continued on next page*)

Table 2 (*continued*)

	Study & year	Study type (CL/FS)[A]	Anatomy Identification	Tool tracking	Tracking system for probe	Probe type
		CL ($n=60$)		Probe localization through sensors on robotic arm	NS	
	Rao et al. (2013)	CL ($n=5$)	CEUS to detect vascularization And CT angiogram to create a 3D model of ROI	Probe localization through sensors on robotic arm	Probe localization through sensors on robotic arm	CEUS
Adrenalectomy	Kumar et al. (2009), Asher et al. (2011)	CL ($n=1$)	Visual inspection for intra-operative tumour boundary detection	Probe localization through sensors on robotic arm	NS	LUS
		CL ($n=12$)			NS	
Cardiac surgery	Wang et al. (2012), (2013)	CL ($n=129$)	Visual inspection to detect cannulae	Probe localization through sensors on robotic arm	NS	TEE
	Suematsu et al. (2007)	FS ($n=10$ pig hearts)	Target and tools identification by visual inspection	Probe localization through sensors on robotic arm	NS	3D TEE

Inclusion criteria: In the referenced studies ultrasound is used to guide robotic surgery at a clinical or feasibility study.
[A] FS = Feasibility study; CL = Clinical study
[C] NS = Not specified.

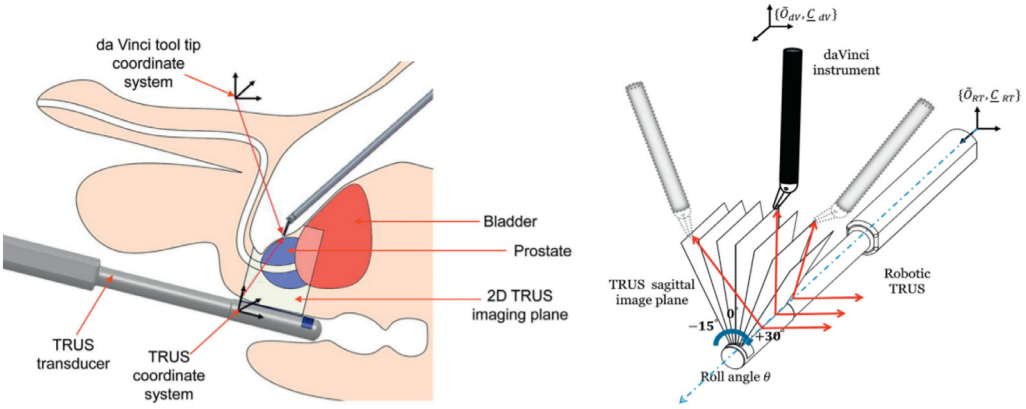

Fig. 5. TRUS rotation to automatically track da Vinci instrument tip (Mohareri et al., 2014).

ables the surgeon to visualize the structures present behind those that can be viewed from the camera in one single image. Different strategies have been used to track the laparoscope and the LUS. Cheung, Wedlake, Moore, Pautler, & Peters (2010) used EM tracking for real-time localization of the images in the two modalities. Hughes-Hallett et al. (2014), Zhang et al. (2017), Edgecumbe and Singla et al. (2016), Singla, Edgcumbe, Pratt, Nguan, & Rohling (2017) used real-time optical pattern tracking. To allow for image fusion, the US probe should be in the laparoscope field of view and can be tracked using a checkerboard pattern fixed on the LUS. In the latter study an additional component with a checkerboard pattern was placed near the tumour to track its location during the dissection while the LUS was not in use and visual clues were used to warn the surgeon about the tumour proximity. Another solution for image augmentation using the checkerboard pattern was proposed by Schneider, Nguan, Rohling, & Salcudean (2016) that instead used LUS to identify the blood vessels and register the US image to a preoperative CT. These studies evaluated the surgeon performance simulating the robotic-assisted surgery on phantoms and ex-vivo models.

A common practice before kidney tumour removal is hilar clamping, which involves clamping the main vessels surrounding the kidney to interrupt blood flow to the organ, to create a bloodless surgical site for intervention (Cabello et al., 2009). However, since this practice can impart severe ischemic injuries to the kidney, several studies suggested alternative "zero-ischemia" methods. To this end, Gill et al. (2011) and Papalia et al. (2012) proposed pharmaceutically-induced hypotension, monitoring blood flow with colour-Doppler US. Rao et al. (2013) introduced the concept of selective clamping, where the region to be devascularized was defined using contrast-enhanced ultrasound (CEUS) (Fig. 6).

The major advantage of CEUS is that the image is not affected by probe motion, which generates false-positives in colour-Doppler mode. In this study, a preoperative CT angiogram was used as well to create a 3D model of vessels, tumour and kidney for planning and to provide a navigation map of the vessel branches during surgery, an approach which had been explored in previous studies (Lasser et al., 2012; Ukimura et al., 2012).

3.3. Teleoperated systems for cardiac surgery

Also in cardiac robotic assisted surgery operations are typically performed using the Da Vinci surgical system (Table 2). The procedures are guided by an endoscopic camera and by intra-cardiac or transesophageal echocardiography (TEE), which plays an important role in monitoring and guiding several steps of the intervention, in particular for mitral valve repair (Vernick and Atluri, 2013) (Fig. 7).

In this type of surgery, as for other intra-cardiac procedures, the most common approach to guarantee endoscopic visualization of the anatomical structures is to establish a cardiopulmonary bypass (CPB), suspending temporarily heart and lung functions (Wang et al., 2012; Wang et al., 2011; Suematsu et al., 2007). A TEE US probe is inserted under general anaesthesia down the esophagus placing the probe tip on the posterior heart wall. Before proceeding with the intervention, CPB is performed via percutaneous, peripheral or central cannulation (Vernick and Atluri, 2013; Ikhsan et al., 2018). The cannulae are guided in the vessels and in the aorta by direct visualization of the wires on 2D US images, where they appear as two parallel, hyperechoic lines (Wang et al., 2012; Wang et al., 2013). However, since CPB has important reported side-effects, such as microemboli formation, inflammation, etc (Suematsu et al., 2007; Yuen et al., 2008), several studies in-

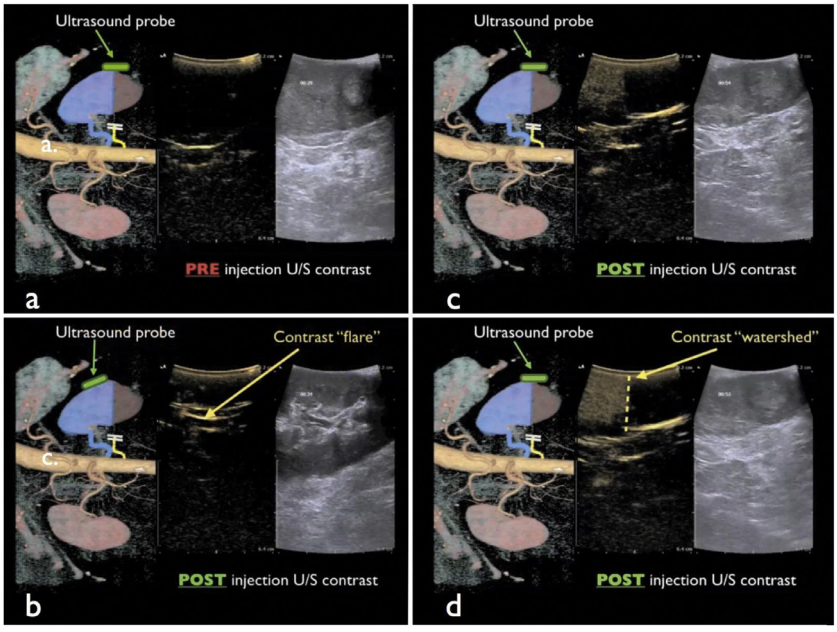

Fig. 6. US image changes pre/post US contrast injection. Each figure shows: on the left, 3D reconstruction based on CT with the respective probe position (green), in the middle CEUS mode image, on the right the US standard image. In each of the 3D anatomy reconstruction the perfused liver is shown in blue, whereas the nonperfused part, due to artery clamping (shown as two white lines) is represented as a grey region. Prior to the injection (Figure a), in the CEUS mode image, the entire kidney appears dark. After the injection (Figure b), in CEUS mode a contrast flare indicates the presence of the supplied blood vessels in the perfuse kidney part. Moving the US probe toward the nonperfused kidney part (Figure c and d) a clear distinction can be made between the two kidney parts, separated by a definite "watershed" (Rao et al., 2013).

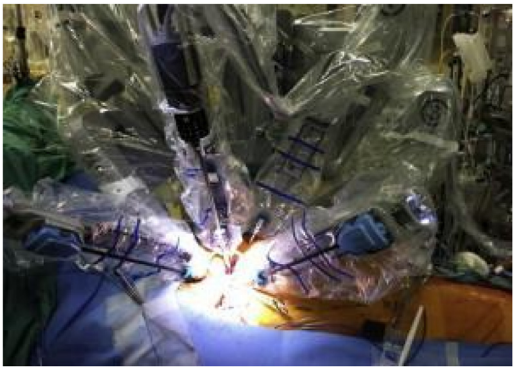

Fig. 7. Robotic-assisted mitral valve repair with robotic arms in the surgical site (Vernick and Atluri, 2013).

vestigated the possibility to use 3D US to visualize the surgical site without removing blood flow and thus avoid CPB.

Suematsu et al. (2007) performed closure of atrial septal defect under 3D US sole guidance on 10 pig hearts using a customized visualization platform. Despite a limited spatial resolution, the anatomical visualization was adequate to perform the surgical task. Other studies focussed on monitoring heart beating motion using 3D US and compensating with a robotic instrument (Yuen et al., 2008; Bowthorpe et al., 2014; Cheng et al., 2018) or with robotic catheters (Kesner and Howe, 2011b). With these techniques, the surgeon could visualize and operate on the heart as if it was static.

Another clinical application for robotic cardiac surgery has been experimented as an alternative to open heart surgery for foreign body removal (Thienphrapa et al., 2011; Thienphrapa et al., 2012). In this study, a small steel ball was inserted in a heart phantom, with simulated cardiac motion. A robotic arm (LARS) (LaRose et al., 1995) was successfully tracked and guided using 3D TEE towards the moving ball, identified on the US images using 3D normalized cross-correlation.

4. US for surgical tool detection

A key component of US-guided autonomous robotic surgical systems is the capability of knowing in real-time the position and orientation of the surgical tool with respect to the anatomy. In these systems, safe closed-loop control is enabled by US-based navigation in the anatomy and tracking of the surgical tools. To this end, specific calibration procedures (Aalamifar et al., 2014) between the US and the robotic systems must be performed, typically using registration techniques (Maintz and Viergever, 1998).

Surgical tools with straight rigid shafts are widely used in surgeries, as they are easy to manipulate and have good force transmission ability. However, the rigidity of the tools drastically limits their range of access when being inserted into the human body. To improve the reachability and dexterity, flexible surgical tools have been developed and are gaining increasing popularity. However, detection of these tools poses significant challenges due to their variable geometry.

Typical examples include steerable needles (Burdette et al., 2010), active cannulas (Swaney et al., 2012), as shown in Fig. 8.

In the next sections, the techniques for detecting straight/flexible surgical tools used in US-guided robotic surgeries are extensively reviewed.

4.1. Straight tools

Detecting straight tools in US images is relatively easy due to the simple geometry of the tools. A common solution is to first digitize the US image into a binary image using a threshold filter and then apply some line detection algorithms. Artefacts are not infrequent in US, though, possibly causing false detection (Hongliang et al., 2011). Therefore, only very robust algorithms should be considered for this task. The Hough Transform (HT) based line detection algorithm was proposed in litera-

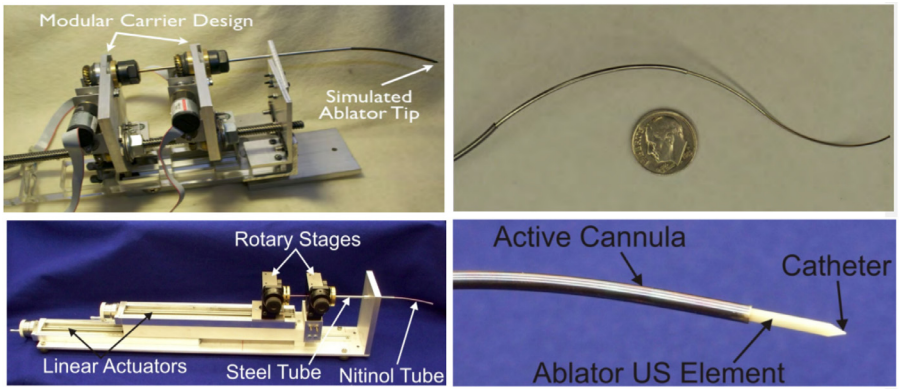

Fig. 8. Examples of flexible surgical tools used in minimally invasive surgery under US guidance. Top Figure: Example of robotic system for steerable needle actuation (on the Left) and steerable needle (on the Right) (Burdette et al., 2010). Bottom Figure: Example of robotic system for active cannula actuation (on the Left) and active cannula (on the Right) (Swaney et al., 2012).

ture (Duda and Hart, 1972). The algorithm is simple but robust, because it converts the complex detection problem in the image space into an easier peak detection problem in the HT space. It is particularly efficient in the case of discontinuous lines, that often appear in US images typically because of artefacts such as shadowing and speckle. Zhou et al. (2008) and Qiu et al. (2013) developed a 3D Improved HT algorithm for automatic needle detection. Volume cropping based on *a priori* knowledge of the needle insertion pose and coarse-fine search strategy were used to improve the computation efficiency. Water phantom experiments showed a position deviation of less than 2 mm and an angular deviation of less than 2°, with a computational time of less than 2 s for a $(381 \times 381 \times 250)$ voxel image. Novotny et al. (2007) proposed a 3D Radon Transform (the continuous form of HT) based algorithm which could calculate the direction and location of the axis of a surgical tool. To further determine the rotational position of the tool around its axis and the position of its tip, passive markers (Stoll et al., 2012) were designed and attached to the distal end of the tool. They reported a tool orientation error of 1.1° and a tip position error of less than 1.8 mm in a water tank experiment. Parallel computing implementation on GPU helped the algorithm reduce detection time to 31 ms. A similar technique based on Parallel Integration Transform (sometimes referred to as X-ray transform) was used for straight electrodes localization (Barva et al., 2008). The localization accuracy was between 0.2 mm and 0.3 mm in several experiments. However, the reported processing time was tens of minutes, partially due to the MATLAB implementation, which was sub-optimal for real-time applications.

Uhečírk et al. (2010) proposed a different approach based on model-fitting and on an expanded version of the random sample consensus (RANSAC) method. Experiments on synthetic and clinical data showed an accuracy better than 1 mm and a MATLAB implementation required less than 1 s in each processing, showing promise for real-time implementation in a compiled language.

Beigi et al. (2016) presented a novel approach to detect a hand-held needle in US-guided interventions by analysing the motion pattern of the needle caused by tremors. The method was evaluated *in vivo* on porcine tissue with mean, SD, and RMS error of 2.83°, 1.64° and 3.23°, respectively.

To enhance the robustness of needle-tip localisation, Mari et al. (2014) integrated an optical fibre hydrophone into the needle cannula and proposed a method to detect the ultrasound pulses based on the maximum and the centroid of the optical fibre hydrophone signal. Xia et al. (2017) and (2016) applied this technology to the US-guided needle tracking for fetal interventions, and achieved an accuracy of 0.39 ± 0.19 mm in the axial dimension and 1.85 ± 0.29 mm in the lateral dimension in a water phantom. Preliminary tests were also performed in an *in vivo* fetal sheep model (Beigi et al., 2016).

Recently, learning based techniques have also been used for needle detection. Beigi et al. (2017) developed a two-step framework for the detection of an invisible needle based on probabilistic support vector machines and time-domain features. An average accuracy of (2.12°, 1.69 mm) and $81\% \pm 4\%$ for localisation and classification in *in vivo* tests was reported (Beigi et al., 2016). Pesteie et al. (2018) proposed a hybrid machine learning system combining a deep network architecture and a feature augmentation technique for needle target localisation in US-guided epidural injections. Average lateral and vertical errors of 1 mm and 0.4 mm were achieved on the planes of 3-D test data, while on 2-D test data, the average lateral and vertical errors were 1.7 mm and 0.8 mm, respectively.

4.2. Steerable needles

Among the advantages of thin percutaneous needles with respect to straight tools are: less deformation of tissue, reduced trauma to patients and larger steerability (Abayazid et al., 2013). The latter in particular is produced by the interaction between the needle and the tissue into which the needle is inserted. Due to the asymmetric bevel-tip with which most needles are designed, the forces exerted on the two sides of the tip are also asymmetric when the needle penetrates through the tissue, creating a curvilinear insertion path. By controlling the rotation angle of the needle along the path, it is possible to reach a target position through a tortuous trajectory and bypass some critical tissues or obstacles (Adebar et al., 2014). Flexible needles have been widely used in biopsies, brachytherapy, blood sampling, etc. (Abolhassani et al., 2007).

The previously mentioned HT based algorithms can also be modified for flexible needle detection as long as the shape of the needle can be appropriately parameterized. Okazawa et al. (2006) demonstrated that the standard HT combined with a polynomial regression was suitable for mildly curved needle detection. For larger curvatures, they proposed to use a set of coordinate transform to adjust the estimated trajectory and then use the HT with a new parameterization based on the assumption of constant radius trajectory. Tests on US images showed a mean error of the tip detection smaller than 1 mm. Processing time was not reported. Neshat and Patel (2008) parameterized the curved needle with a Bézier polynomial that is compatible with inconstant radius curves. A 2D laparoscopic US transducer was attached to a robotic probe holder to generate 3D images by

rotating around the transducer axis. A GPU-based algorithm was implemented to speed up processing time up to about 20 times faster than the CPU-based one. Aboofazeli et al. (2009) proposed a two-step method for 3D curved needle detection. First, they projected the needle onto a 2D plane, and found the surface that the projection of the needle formed in the 3D volume; then, they flattened the surface on which the needle was located and detected the needle using a HT followed by polynomial curve fitting. The average error in needle tip detection was smaller than 2.8 mm and the segmentation for a $(256 \times 256 \times 125)$ voxel image took around 3 s.

A research team from the University of Twente (Abayazid et al., 2014, 2013; Moreira and Misra, 2015; Vrooijink et al., 2013) developed a real-time 3D flexible needle steering system where only the tip position of the needle was tracked using a high-resolution 2D US transducer, placed perpendicular to the needle insertion direction. A HT based algorithm was then developed to determine the location of the needle on the US image while cancelling the comet tail artefact. A positioning device was used to move the transducer to keep tracking the needle tip while it traversed the tissue. A needle deflection model was integrated to assist steering, and a targeting accuracy of 0.42 mm was achieved in soft-tissue phantom experiments. Neubach and Shoham (2010) also used a 2D US transducer to track the needle tip; the location of the needle tip was detected by image subtraction on consecutive frames. The closed-loop experiment demonstrated a needle-tip tracking error of around 1 mm.

In contrast to the previously described approaches, Adebar et al. (2014) and Housden et al. (2012) used Doppler US for curved needle detection. An external actuator was implemented to vibrate the needle with a low-amplitude high-frequency motion. This could be detected by the (Duplex) Doppler system which showed position and shape of the needle, avoiding this way complex segmentation procedures. An average error of 1.57 mm in steering a needle tip to a simulated target was reported with this method.

4.3. Active cannulas

Active cannulas, also called concentric tube robots, are another class of steerable tools developed recently for MIS applications (Swaney et al., 2012). Different from flexible needles, whose deformation relies on the interaction with their surrounding tissues, active cannulas have the capability to actively change their morphology and tip pose. These flexible tools usually consist of two to three concentric tubes whose diameters range from sub-mm to mm. The tubes are nested one by one and independently held at their proximal ends. By rotating and translating each tube, abundant variations of the entire shape of the tubes can be achieved. As such, active cannulas have the capability to navigate along complex 3D paths inside the human body via small open orifices or incisions, while avoiding collision with tissues along the slender passage thanks to their relatively high rigidity. To date, different procedures have been proposed for active cannulas such as intra-cardiac procedures (Nadeau et al., 2015), liver ablation (Burdette et al., 2010), intraocular procedures (Wu et al., 2015a), and transnasal surgery (Wu et al., 2016).

Active cannulas share many similar characteristics with steerable needles such as material and diameter. Therefore, many of the introduced algorithms for detecting steerable needles on 3D US are applicable to active cannulas as well. Nonetheless, there are just a few works taking active cannulas as their focus applications. Nadeau et al. (2015) developed an intensity-based visual servoing framework for tracking active cannulas in 3D US volumes. The direct use of image intensity information removed the need for primitive extraction or image segmentation and improved the computational efficiency (Nadeau et al., 2015). Experiments on a porcine model during a robotic beating-heart Patent Foramen Ovale closure procedure were conducted to demonstrate the feasibility of the proposed framework. The image processing was able to run at the real-time rate of 25 Hz; the accuracy, however, was not reported.

Ren et al. (2011) proposed an approach similar to the one Aboofazeli et al. (2009) used for curved line detection, but including a five-step pipeline for pre-processing, a RANSAC algorithm for plane detection, and a circle-fitting algorithm. In subsequent work, they introduced a tubular enhanced geodesic active contours method (Hongliang and Dupont, 2013; Ren and Dupont, 2011) based on the multiscale vessel enhancement filtering technique developed in Frangi et al. (1998) to replace the pre-processing step. Recently, Ren et al. (2017) demonstrated that by simply varying the US power level, it is possible to identify high acoustic impedance robotic instruments in low-quality US images.

4.4. Steerable catheters

Steerable catheters are a third type of flexible tools widely used in particular in cardiac surgery. These catheters usually have a built-in cable-driven mechanism: the tip of the catheter can be steered by connecting cables to the tip of the catheter and actuating the cables at the proximal end. Multiple bending sections that enable S-shapes can be realised by increasing the number of independent controllable segments and associated actuating cables. Steerable catheters are usually long and thin, with a length from sub-m to m and a diameter from sub-mm to mm. In a typical cardiac catheterization, the catheter is inserted through a small incision in the patient's neck, arm, or groin into the vascular system to reach the heart for ablation, electrical activity measurement or observation (Wu et al., 2015b). Due to the complexity in steering the catheters during the surgery, robotic catheter systems have been developed that can improve the efficiency, compensate for the heartbeat motion, and protect surgeons from radiation (Kesner and Howe, 2011a).

Since steerable catheters can be in both straight and curved shapes during a procedure, algorithms that are capable of detecting both shapes are preferable. Kesner et al. (Kesner, 2014; Kesner and Howe, 2011a) developed a robotic catheter system for 3DUS-guided cardiac ablation. The system included active motion compensation in one degree of freedom and force control on the catheter tip. The system used US only to track the tip section of the catheter during the procedure, assuming that this section was always straight. A GPU-based Radon Transform algorithm tracked the catheter axis (Novotny et al., 2007). Reddy et al. (2008) demonstrated that colour Doppler US could provide image guidance for cardiac catheters.

Wu et al. (2015b) pointed out that TEE, although providing rich soft tissue information, has a limited FOV that prevents detection of the entire catheter. They therefore proposed to combine the modality with X-ray fluoroscopy for catheter segmentation. A framework consisting of four modules was developed: 1) catheter extraction from the initial X-ray frame; 2) catheter tracking on the following X-ray frames; 3) X-ray and US registration; and 4) catheter extraction from US. Particularly, search space straightening and speeded up robust features (SURF) extraction were used in the last module to first determine the 2D plane of the catheter and then localize the catheter in that plane, similarly as (Aboofazeli et al., 2009). Tests on both porcine data and patient data showed that they were able to track the catheter at 1.3 s per frame, with an error smaller than 2 mm. However, the algorithm still needed further development for real-time clinical applications.

5. Discussion

Two main groups of applications, at either clinical or experimental level, in the past decade have been identified in US-guided minimally invasive robotic interventions: percutaneous needle procedures and robotic-assisted MIS. The latter group consists mainly in tele-operated robotic applications, as a direct evolution of MIS (Lanfranco et al., 2004). For these types of applications, the surgical procedure does not change, but the surgeons operate on the patient using robotic arms, that can correct for instabilities and can produce highly precise motion (Leven et al., 2005). All the most recent improvements introduced in this field aimed at providing extra-feedback to the surgeon, rather than introducing automation. For example, the use of elastography to transfer haptic feedback to the surgeon in order to sense tumoural masses, as in open surgery (Schneider et al., 2012a; Deshmukh et al., 2014); or the introduction of enhanced visualization interfaces, such as in partial nephrectomy (Rao et al., 2013). This is due to the complexity of these procedures in terms of decision making and actions to be performed (Lanfranco et al., 2004), which still require human interaction and make dexterity and accuracy enhancement a priority over automation. But it is also due to the limited real-time quantitative anatomical information provided to the system by the available imaging modalities implemented. This information could possibly enable autonomous operation.

For percutaneous needle procedures, instead, almost every system developed in the past ten years was either autonomous or semi-autonomous (Table 1). It must be noted though that only a few semi-autonomous systems were tested in clinical studies. The enhanced degree of automation for these systems was facilitated by the limited number of systematic steps in these types of procedure, by the absence of complex decisions and by the ease in reaching the surgical site. For example, once the target and the entry point for the biopsy needle are defined, the needle will follow a straight path, reach the target and exit along the same path. It must be noted, though, that in the works reviewed the intra-operative motility of the organs was generally underestimated. In semi-autonomous systems, in fact, target tracking was usually not taken into account under the main assumption that, whenever organ motion would occur, the clinician would detect the motion using real-time imaging and would compensate for it. Even among the autonomous systems developed, only few works considered organ motion for needle path correction (Mallapragada et al., 2008; Hungr et al., 2009; Long et al., 2012a). Moreover, in these studies the systems were tested on phantoms, hence not accounting for tissue inhomogeneity and possible complex deformations present in human tissues, thus oversimplifying the identification and the tracking task of the structure of interest. Although many algorithms for US automatic segmentations and registration have been developed, accurate soft tissue tracking is still challenging, mostly due to the limited FOV of US images and to their sensitivity to probe orientation/position. In order to provide the robot with a larger, more consistent FOV, several studies developed tracking algorithms combining MRI and US, either implementing rigid/deformable registration (Sonn et al., 2014; Ukimura et al., 2015; Zhang et al., 2016) or, more recently, trying to simulate real-time MRI based navigation using the information from the US datasets (Preiswerk et al., 2016). In general, intraoperative navigation in US volumes is still a challenging objective, in particular in robot-assisted laparoscopic surgery which is currently the only clinical operating modality where vision systems (endoscopic cameras) are combined with US. Intuitive visualization of structures in US images, and easily interpretable fusion with the endoscopic video are complex tasks. The endoscopic view is a 2D surface in a 3D space which needs to be localized with respect to US. But the two modalities are typically not tracked in the same coordinate system, so it is necessary to apply advanced image processing techniques to identify the same structures in the two modalities and overlap them (Ukimura & Gill, 2009). Moreover, laparoscopic applications often use internal US probes, with limited FOV especially if compared to open surgery (Edgcumbe et al., 2016). Several authors suggest augmented reality might be a possible solution to overcome these limitations and improve operating conditions (Singla et al., 2017). It must be noted that most clinical applications presently implement 2D US, which only shows one plane which must be aligned manually with the anatomy to visualize. If there are significant anatomical changes off plane, with these technologies it is really difficult to take the deformations into account. In some cases, volumes can be reconstructed sweeping the 2D US across the region of interest. But it is a relatively slow process which might produce important geometric aberrations in case deformations happen whilst sweeping. Recently, though, 3D/4D US has become a standard in diagnostic imaging. In particular, phased array probes scan full volumes with large FOV and with fast refresh rates (up to 6 Hz full volumetric refresh or even more) that can reliably show possible anatomical deformations in real time.

From the studies reported here it is clear that US, despite it being a very mature technology for diagnostic and radiological applications, for quantitative localization or tissue characterization purposes still needs much development. In particular, autonomous applications require automatic interpretation of images, which is a relatively novel field of research, especially for US (Camps et al., n.d.). Most innovative works implement relatively new technologies and are at the proof-of-concept stage mainly on phantoms, where algorithms perform well. But translation into clinic is very complex, and validation of algorithms on real cases require important efforts and time. Among the technologies reviewed, only the teleoperated ones have made their way into the clinics, because the workflow followed is the same as in standard procedures, so adoption was easier. In particular, it is difficult to accept for clinicians to completely give up control on some or even every step of the procedures. Autonomous and semi-autonomous systems, are not widespread because they require as previously stated very high levels of automation, especially in image processing, which are not yet available. In this review, the main focus was on the imaging aspects, but also other components in these complex systems may impose severe limitations: for example, it is difficult to estimate the final tracking accuracy in a chain where possibly robotic components, localization devices and imaging aberrations need to be combined. Moreover, time delays among the different sub-systems, communication consistency and, above all, safety of operation also need to be managed properly. Also quality assurance for the whole procedure is complex to envision.

Applications using machine learning have been proposed to increase the degree of automation in these procedures, by automatically identifying and tracking anatomical structures, for example the left ventricle endocardium (Venkates et al., 2015). Machine learning approaches are particularly promising as they can recognize similar patterns in images with significant variations in quality and appearance (Noble, 2010). They also hold promise for automatic US image interpretation, for diagnostic applications (Lempitsky et al., 2009; Venkates et al., 2015; Carneiro et al., 2008) but also for autonomous identification of tumoural tissues for guidance in surgical and/or ablative robotic resections.

Another interesting area where the tissue typing/tissue characterization capabilities of US (in particular for soft tissues like muscles, tendons, vessels, nerves and internal organs (Carovac et al., 2011)), in combination with robotics, could potentially be beneficial is “keyhole” surgery in orthopaedics (e.g. arthroscopy) (Zheng and Nolte, 2015). The currently existing robotic technol-

ogy for orthopaedic surgical assistance is restricted to those procedures (such as total knee arthroplasty) where navigation information is limited to bony structure (Picard et al., 2016). Accurate soft-tissue tracking might expand the use of robots in this field, possibly reducing human errors, side-effects, interventional time, operator dependence and surgeon learning curve and fatigue (Reigstad and Grimsgaard, 2006; de Steiger et al., 2015). For more complex and/or deep anatomical structures, such as shoulders or hips, 2D US spatial limitations (information is provided only on a plane) might make this imaging modality insufficient. In these cases, volumetric imaging, possibly in real-time (4D imaging), might be necessary to effectively monitor organ deformations in response to tool penetration in the anatomy and/or to avoid critical anatomical structures (e.g. vessels, nerves) in the surgical site. It should be noted that presently, to our knowledge, no volumetric real-time imaging other than US, recently introduced in clinical practice, can be implemented for these procedures, because of the operating theatre requirements.

Apart from tracking the anatomy during the intervention, the robotic system should also be aware of the position of the surgical tool. In the clinical applications analysed, the surgical instrument used (needles and shafts) were usually rigid, and thus easy to track. However, flexible/continuum robots might be used to enhance the tool manoeuvrability. In these cases, tracking can become challenging and many sensors might be needed to provide detailed information about the location of the entire tool. US holds potential also to detect the shape of the tool and, by providing this information to the tracking system, help localize it.

6. Conclusions

US is widely used in several robotic applications in MIS to identify, localize, segment and track regions of interest and operating tools. This imaging modality has real time capabilities, is compatible with operating theatres and is harmless for the patient, all unique characteristics making it an important component in future advancements of robotic systems, possibly fulfilling the requirements for autonomous systems implementation. Among the reviewed studies, the majority of the systems where a higher level of automation was implemented were at the proof-of-concept level, and significant developments are still necessary before they can be translated into the clinic. 3D/4D US technology, combined with tracking techniques such as image registration, image-fusion and machine learning, is very promising and should be further explored. The final aim to provide a detailed dynamic map of the surgical site to make autonomous robots a possible and safe interventional option seems to be within reach, but it is paramount to make US interpretation automatic.

Funding

This work was supported by the grant from the Australia-India Strategic Research Fund (2016001729).

References

Aalamifar, F., Khurana, R., Cheng, A., Taylor, R.H., Iordachita, I., Boctor, E.M., 2014. Enabling technologies for robot assisted ultrasound tomography: system setup and calibration. Proc. SPIE 9040, 90401X. https://doi.org/10.1117/12.2045516.

Abayazid, M., Roesthuis, R.J., Reilink, R., Misra, S., 2013. Integrating deflection models and image feedback for real-time flexible needle steering. IEEE Trans. Robot. 29, 542–553. https://doi.org/10.1109/TRO.2012.2230991.

Abayazid, M., Vrooijink, G.J., Patil, S., Alterovitz, R., Misra, S., 2014. Experimental evaluation of ultrasound-guided 3D needle steering in biological tissue. Int. J. Comput. Assist. Radiol. Surg. 9, 931–939. https://doi.org/10.1007/s11548-014-0987-y.

Abolhassani, N., Patel, R., Moallem, M., 2007. Needle insertion into soft tissue: a survey. Med. Eng. Phys. https://doi.org/10.1016/j.medengphy.2006.07.003.

Aboofazeli, M., Abolmaesumi, P., Mousavi, P., Fichtinger, G., 2009. A new scheme for curved needle segmentation in threedimensional ultrasound images. In: Proc. - 2009 IEEE Int. Symp. Biomed. Imaging From Nano to Macro. ISBI, pp. 1067–1070. 2009 https://doi.org/10.1109/ISBI.2009.5193240.

Aboumarzouk, O.M., Stein, R.J., Eyraud, R., Haber, G.-P., Chlosta, P.L., Somani, B.K., Kaouk, J.H., 2012. Robotic versus laparoscopic partial nephrectomy: a systematic review and meta-analysis. Eur. Urol. 62, 1023–1033. https://doi.org/10.1016/j.eururo.2012.06.038.

Adebar, T.K., Fletcher, A.E., Okamura, A.M., 2014. 3-D ultrasound-guided robotic needle steering in biological tissue. IEEE Trans. Biomed. Eng. 61, 2899–2910. https://doi.org/10.1109/TBME.2014.2334309.

Adebar, T.K., Okamura, A.M., 2013. 3D segmentation of curved needles using Doppler ultrasound and vibration. Lect. Notes Comput. Sci. 61–70. (including Subser. Lect. Notes Artif. Intell. Lect. Notes Bioinformatics) 7915 LNCS https://doi.org/10.1007/978-3-642-38568-1_7 .

Antoniou, S.A., Antoniou, G.A., Antoniou, A.I., Granderath, F.-A., 2015. Past, present, and future of minimally invasive abdominal surgery. JSLS J. Soc. Laparoendosc. Surg. 19 https://doi.org/10.4293/JSLS.2015.00052.

Araujo, R.L.C., de Castro, L.A., Fellipe, F.E.C., Burgardt, D., Wohnrath, D.R., 2017. Robotic left lateral sectionectomy as stepwise approach for cirrhotic liver. J. Robot. Surg. 0–3. https://doi.org/10.1007/s11701-017-0730-0.

Asher, K.P., Gupta, G.N., Boris, R.S., Pinto, P.A., Linehan, W.M., Bratslavsky, G., 2011. Robot-assisted laparoscopic partial adrenalectomy for pheochromocytoma: the national cancer institute technique. Eur. Urol. 60, 118–124. https://doi.org/10.1016/j.eururo.2011.03.046.

Azizian, M., Khoshnam, M., Najmaei, N., Patel, R.V., 2014. Visual servoing in medical robotics: a survey. Part I: endoscopic and direct vision imaging – techniques and applications. Int. J. Med. Robot. Comput. Assist. Surg. MRCAS 10, 263–274. https://doi.org/10.1002/rcs.

Barva, M., Uherčík, M., Mari, J.-M., Kybic, J., Duhamel, J.-R., Liebgott, H., Hlavac, V., Cachard, C., 2008. Parallel integral projection transform for straight electrode localization in 3-D ultrasound images. IEEE Trans. Ultrason. Ferroelectr. Freq. Control 55, 1559–1569.

Bassan, H., Hayes, T., Patel, R.V, Moallem, M., 2007. A novel manipulator for 3D ultrasound guided percutaneous needle insertion. In: 2007 IEEE Int. Conf. Robot. Autom., pp. 10–14. https://doi.org/10.1109/ROBOT.2007.363055.

Baumann, M., Mozer, P., Daanen, V., Troccaz, J., 2007. Towards 3D ultrasound image based soft tissue tracking: a transrectal ultrasound prostate image alignment system. Med. Image Comput. Comput. Interv. 2007, Part II 26–33 https://doi.org/10.1007/978-3-540-75759-7_4 .

Besl, P.J., McKay, Neil D., 1992. A method for registration of 3-D shapes. IEEE Trans. Pattern Anal. Mach. Intell. 14, 239–256.

Bhayani, S.B., Snow, D.C., 2008. Novel dynamic information integration during da Vinci robotic partial nephrectomy and radical nephrectomy. J. Robot. Surg. 2, 67–69. https://doi.org/10.1007/s11701-008-0083-9.

Billings, S., Deshmukh, N., Kang, H.J., Taylor, R., Boctor, E.M., 2012. System for robot-assisted real-time laparoscopic ultrasound elastography. Med. Imaging 2012 Image-Guided Proced. Robot. Interv. Model. 8316 https://doi.org/10.1117/12.911086.

Boctor, E.M., Choti, M.A., Burdette, E.C., Webster, R.J., 2008. Three-dimensional ultrasound-guided robotic needle placement: an experimental evaluation. Int. J. Med. Robot. Comput. Assist. Surg. MRCAS 4, 180–191. https://doi.org/10.1002/rcs.

Boukerroui, D., Basset, O., Baskurt, a., Gimenez, G., 2001. A multiparametric and multiresolution segmentation algorithm of 3-D ultrasonic data. IEEE Trans. Ultrason. Ferroelectr. Freq. Control 48, 64–77. https://doi.org/10.1109/58.895909.

Bowthorpe, M., Tavakoli, M., Becher, H., Howe, R., 2014. Smith predictor-based robot control for ultrasound-guided teleoperated beating-heart surgery. IEEE J. Biomed. Heal. Informatics 18, 157–166. https://doi.org/10.1109/JBHI.2013.2267494.

Burdette, E.C., Rucker, D.C., Prakash, P., Diederich, C.J., Croom, J.M., Clarke, C., Stolka, P., Juang, T., Boctor, E.M., Webster III, R.J., 2010. The ACUSITT ultrasonic ablator: the first steerable needle with an integrated interventional tool. Proc. SPIE Med. Imaging. 7629, 76290V–76290V–10 https://doi.org/10.1117/12.845972.

Cabello, J.M., Benway, B.M., Bhayani, S.B., 2009. Robotic-assisted partial nephrectomy: surgical technique using a 3-arm approach and sliding-clip renorrhaphy. Int. Braz J Urol 35, 199–204. https://doi.org/10.1590/S1677-55382009000200010.

Calin, M.L., Sadiq, A., Arevalo, G., Fuentes, R., Flanders, V.L., Gupta, N., Nasri, B., Singh, K., 2016. The first case report of robotic multivisceral resection for synchronous liver metastasis from pancreatic neuroendocrine tumor: a case report and literature review. J. Laparoendosc. Adv. Surg. Tech. 26, 816–824. https://doi.org/10.1089/lap.2016.0342.

Carneiro, G., Georgescu, B., Good, S., Comaniciu, D., 2008. Detection and measurement of fetal anatomies from ultrasound images using a constrained probabilistic boosting tree. IEEE Trans. Med. Imaging 27, 1342–1355. https://doi.org/10.1109/TMI.2008.928917.

Carovac, A., Smajlovic, F., Junuzovic, D., 2011. Application of ultrasound in medicine. Acta Inform. Medica 19, 168. https://doi.org/10.5455/aim.2011.19.168-171.

Cheng, L., Sharifi, M., Tavakoli, M., 2018. Towards robot-assisted anchor deployment in beating-heart mitral valve surgery. Int. J. Med. Robot. Comput. Assist. Surg. https://doi.org/10.1002/rcs.1900.

Chopra, S., Dinshaw, K., Kamble, R., S., R., 2006. Breast movement during normal and deep breathing, respiratory training and set up errors: implications for external beam partial breast irradiation. Br. J. Radiol. 79, 766–773. https://doi.org/10.1259/bjr/98024704.

De Silva, T., Bax, J., Fenster, A., Samarabandu, J., Ward, A.D., 2011. Quantification of prostate deformation due to needle insertion during TRUS-guided biopsy: comparison of hand-held and mechanically stabilized systems. Med. Phys. 38 https://doi.org/10.1117/12.878359.

de Steiger, R.N., Liu, Y.-L., Graves, S.E., 2015. Computer navigation for total knee arthroplasty reduces revision rate for patients less than sixty-five years of age. J. Bone Jt. Surg.-Am. 97, 635–642. https://doi.org/10.2106/JBJS.M.01496.

Deshmukh, N.P., Kang, H.J., Billings, S.D., Taylor, R.H., Hager, G.D., Boctor, E.M., 2014. Elastography using multi-stream GPU: an application to online tracked ultrasound elastography, in-vivo and the da Vinci surgical system. PLoS One. 9 https://doi.org/10.1371/journal.pone.0115881.

DiMaio, S.P., Salcudean, S.E., 2003. Needle insertion modeling and simulation. Ieee Trans. Robot. Autom. 19, 864–875. https://doi.org/10.1109/Tra.2003.817044.

Ding, M., Wei, Z., Gardi, L., Downey, D.B., Fenster, A., 2006. Needle and seed segmentation in intra-operative 3D ultrasound-guided prostate brachytherapy. Ultrasonics 44, 331–336. https://doi.org/10.1016/j.ultras.2006.07.003.

Duda, R.O., Hart, P.E., 1972. Use of the Hough transformation to detect lines and curves in pictures. Commun. ACM 15, 11–15. https://doi.org/10.1145/361237.361242.

Dwyer, R.H., Scheidt, M.J., Marshall, J.S., Tsoraides, S.S., 2018. Safety and efficacy of synchronous robotic surgery for colorectal cancer with liver metastases. J. Robot. Surg. https://doi.org/10.1007/s11701-018-0813-6.

Eisele, R.M., 2016. Advances in local ablation of malignant liver lesions. World J. Gastroenterol. 22, 3885–3891. https://doi.org/10.3748/wjg.v22.i15.3885.

Elgezua, I., Kobayashi, Y., Fujie, M.G., 2013. Survey on current state-of-the-art in needle insertion robots: open challenges for application in real surgery. Procedia CIRP 5, 94–99. https://doi.org/10.1016/j.procir.2013.01.019.

El-Serag, H.B.E.L., Rudolph, K.L., 2007. Reviews in basic and clinical gastroenterology. Gastroenterology 132, 2557–2576. https://doi.org/10.1053/j.gastro.2007.04.061.

Faber, K., de Abreu, A.L.C., Ramos, P., Aljuri, N., Mantri, S., Gill, I., Ukimura, O., Desai, M., 2015. Image-guided robot-assisted prostate ablation using water jet-hydrodissection: initial study of a novel technology for benign prostatic hyperplasia. J. Endourol. 29, 63–69. https://doi.org/10.1089/end.2014.0304.

Fenster, A., Downey, D.B., 2001. Three-dimensional ultrasound imaging. Phys. Med. Biol. https://doi.org/10.1117/12.440246.

Fichtinger, G., Fiene, J.P., Kennedy, C.W., Kronreif, G., Song, D.Y., Burdette, E.C., Kazanzides, P., Gmbh, S., 2008. Robotic assistance for ultrasound-guided prostate brachytherapy. Med Image Anal 12, 535–545. https://doi.org/10.1016/j.media.2008.06.002.Robotic.

Fleming, I.N., Kut, C., Macura, K.J., Su, L.-M., Rivaz, H., Schneider, C.M., Hamper, U., Lotan, T., Taylor, R., Hager, G., Boctor, E., 2012. Ultrasound elastography as a tool for imaging guidance during prostatectomy: initial experience. Med. Sci. Monit. 18, CR635–CR642.

Frangi, A.F., Niessen, W.J., Vincken, K.L., Viergever, M.A.. Multiscale vessel enhancement filtering 130–137.

Ghilezan, M.J., Jaffray, D.A., Siewerdsen, J.H., Van Herk, M., Shetty, A., Sharpe, M.B., Jafri, S.Z., Vicini, F.A., Matter, R.C., Brabbins, D.S., Martinez, A.A., 2005. Prostate gland motion assessed with cine-magnetic resonance imaging (cine-MRI). Int. J. Radiat. Oncol. Biol. Phys. 62, 406–417. https://doi.org/10.1016/j.ijrobp.2003.10.017.

Gill, I.S., Eisenberg, M.S., Aron, M., Berger, A., Ukimura, O., Patil, M.B., Campese, V., Thangathurai, D., Desai, M.M., 2011. "Zero ischemia" partial nephrectomy: Novel laparoscopic and robotic technique. Eur. Urol. 59, 128–134. https://doi.org/10.1016/j.eururo.2010.10.002.

Giulianotti, P.C., Buchs, N.C., Coratti, A., Sbrana, F., Lombardi, A., Felicioni, L., Bianco, F.M., Addeo, P., 2011. Robot-assisted treatment of splenic artery aneurysms. Ann. Vasc. Surg. 25, 377–383. https://doi.org/10.1016/j.avsg.2010.09.014.

Hadaschik, B.A., Kuru, T.H., Tulea, C., Rieker, P., Popeneciu, I.V., Simpfendörfer, T., Huber, J., Zogal, P., Teber, D., Pahernik, S., Roethke, M., Zamecnik, P., Roth, W., Sakas, G., Schlemmer, H.P., Hohenfellner, M., 2011. A novel stereotactic prostate biopsy system integrating pre-interventional magnetic resonance imaging and live ultrasound fusion. J. Urol. 186, 2214–2220. https://doi.org/10.1016/j.juro.2011.07.102.

Han, M., Kim, C., Mozer, P., Schäfer, F., Badaan, S., Vigaru, B., Tseng, K., Petrisor, D., Trock, B., Stoianovici, D., 2012. Tandem-robot assisted laparoscopic radical prostatectomy (T-RALP) to improve the neurovascular bundle visualization: a feasibility study. Urology 77, 502–506. https://doi.org/10.1016/j.urology.2010.06.064.Tandem-Robot.

Hemmerling, T.M., Taddei, R., Wehbe, M., Cyr, S., Zaouter, C., Morse, J., 2013. First robotic ultrasound-guided nerve blocks in humans using the magellan system. Anesth. Analg. 116, 491–494. https://doi.org/10.1213/ANE.0b013e3182713b49.

Hill, J.S., McPhee, J.T., McDade, T.P., Zhou, Z., Sullivan, M.E., Whalen, G.F., Tseng, J.F., 2009. Pancreatic neuroendocrine tumors. Cancer 115, 741–751. https://doi.org/10.1002/cncr.24065.

Ho, H., Yuen, J.S.P., Mohan, P., Lim, E.W., Cheng, C.W.S., 2011. Robotic transperineal prostate biopsy: pilot clinical study. Urology 78, 1203–1208. https://doi.org/10.1016/j.urology.2011.07.1389.

Ho, H.S.S., Mohan, P., Lim, E.D., Li, D.L., Yuen, J.S.P., Ng, W.S., Lau, W.K.O., C., C.W.S., 2009. Robotic ultrasound-guided prostate intervention device: system description and results from phantom studies. Int. J. Med. Robot. 5, 51–58. https://doi.org/10.1002/rcs.

Hongliang, R., Dupont, P.E., 2013. Tubular enhanced geodesic active contours for continuum robot detection using 3D ultrasound. Proc. IEEE Int. Conf. Robot. Autom. 1–16. https://doi.org/10.1109/ICRA.2012.6225033.

Hongliang, R., Vasilyev, N.V., Dupont, P.E., 2011. Detection of curved robots using 3D ultrasound. Rep U S 4, 2083–2089. https://doi.org/10.1126/scisignal.2001449.Engineering.

Horsch, K., Giger, M.L., Venta, L.A., Vyborny, C.J., 2002. Computerized diagnosis of breast lesions on ultrasound. Med. Phys. 28, 1652–1659. https://doi.org/10.1118/1.1386426.

Housden, R.J., Arujuna, A., Ma, Y., Nijhof, N., Gijsbers, G., Bullens, R., O'Neill, M., Cooklin, M., Rinaldi, C.A., Gill, J., Kapetanakis, S., Hancock, J., Thomas, M., Razavi, R., Rhode, K.S., 2012. Evaluation of a real-time hybrid three-dimensional echo and X-ray imaging system for guidance of cardiac catheterisation procedures. In: Medical Image Computing and Computer-Assisted Intervention 2012, Part II, pp. 25–32. https://doi.org/10.1007/978-3-642-38568-1_7.

Hruskaa, C.B., O'Connor, M.K., 2008. Quantification of lesion size, depth, and uptake using a dual-head molecular breast imaging system. Med. Phys. 35, 1365–1376. https://doi.org/10.1118/1.2885371.

Hung, A.J., De Castro Abreu, A.L., Shoji, S., Goh, A.C., Berger, A.K., Desai, M.M., Aron, M., Gill, I.S., Ukimura, O., 2012. Robotic transrectal ultrasonography during robot-assisted radical prostatectomy. Eur. Urol 62, 341–348.

Hungr, N., Troccaz, J., Zemiti, N., Tripodi, N., 2009. Design of an ultrasound-guided robotic brachytherapy needle-insertion system. In: Proc. 31st Annu. Int. Conf. IEEE Eng. Med. Biol. Soc. Eng. Futur. Biomed. EMBC 2009, pp. 250–253. https://doi.org/10.1109/IEMBS.2009.5333801.

Ikhsan, M., Tan, K.K., Putra, A.S., 2018. Assistive technology for ultrasound-guided central venous catheter placement. J. Med. Ultrason. https://doi.org/10.1007/s10396-017-0789-2.

Izquierdo-Luna, J.S., Campos-Salcedo, J.G., Estrada-Carrasco, C.E., Torres-Gomez, J.J., Lopez-Silvestre, J.C., Zapata-Villalba, M.A., 2016. Robot-assisted laparoscopic partial nephrectomy with hydrodissection. Actas Urol. Esp. 40, 333–336. https://doi.org/10.1016/j.acuro.2015.11.004.

Kaczmarek, B.F., Sukumar, S., Petros, F., Trinh, Q., Mander, N., Chen, R., Menon, M., Rogers, C.G., 2013. Original article: clinical investigation robotic ultrasound probe for tumor identification in robotic partial nephrectomy: initial series and outcomes. Int. J. Urol. 20, 172–176. https://doi.org/10.1111/j.1442-2042.2012.03127.x.

Kaicheng, L., Rogers, A.J., Light, E.D., von Allmenb, D., Smith, S.W., 2010. Simulation of autonomous robotic multiple-core biopsy by 3D ultrasound guidance. Ultrason. Imaging 32, 118–127.

Kesner, S.B., 2014. Robotic catheter cardiac ablation combining ultrasound guidance and force control. Int. J. Rob. Res. 33, 631–644. https://doi.org/10.1177/0278364913511350.

Kesner, S.B., Howe, R.D., 2011a. Position control of motion compensation cardiac catheters. IEEE Trans. Robot. https://doi.org/10.1109/TRO.2011.2160467.

Kesner, S.B., Howe, R.D., 2011b. Position control of motion compensation cardiac catheters. IEEE Trans. Robot. 86, 1–11. https://doi.org/10.1007/s11103-011-9767-z.Plastid.

König, K., Scheipers, U., Pesavento, A., Lorenz, A., Ermert, H., Senge, T., 2005. Initial experiences with real-time elastography guided biopsies of the prostate. J. Urol. 174, 115–117. https://doi.org/10.1097/01.ju.0000162043.72294.4a.

Kumar, A., Hyams, E.S., Stifelman, M.D., 2009. Robot-assisted partial adrenalectomy for isolated adrenal metastasis. J. Endourol. 23, 651–654.

Lagerburg, V., Moerland, M.A., Jan, J.W., Lagendijk, J.J.B., 2005. Measurement of prostate rotation during insertion of needles for brachytherapy. Radiother. Oncol. 77, 318–323. https://doi.org/10.1016/J.RADONC.2005.09.018.

Lanfranco, A.R., Castellanos, A.E., Desai, J.P., Meyers, W.C., 2004. Robotic surgery. Ann. Surg. 239, 14–21. https://doi.org/10.1097/01.sla.0000103020.19595.7d.

LaRose, D., Taylor, R.H., Funda, J., Eldridge, B., Gomory, S., Talamini, M., Kavoussi, L., Anderson, J., Gruben, K., 1995. A telerobotic assistant for laparoscopic surgery. IEEE Eng. Med. Biol. Mag. 14, 279–288. https://doi.org/10.1109/51.391776.

Lasser, M., Doscher, M., Keehn, A., Chernyak, V., 2012. Virtual surgical planning: a novel aid to robot-assisted. J. Endourol. 26, 1372–1379. https://doi.org/10.1089/end.2012.0093.

Lee, S.L., Lerotic, M., Vitiello, V., Giannarou, S., Kwok, K.W., Visentini-Scarzanella, M., Yang, G.Z., 2010. From medical images to minimally invasive intervention: computer assistance for robotic surgery. Comput. Med. Imaging Graph. 34, 33–45. https://doi.org/10.1016/j.compmedimag.2009.07.007.

Lempitsky, V., Verhoek, M., Noble, J.A., Blake, A., 2009. Random forest classification for automatic delineation of myocardium in real-time 3D echocardiography. In: Proc. 5th Int. Conf. Funct. Imaging Model. Hear., 5528, pp. 447–456. https://doi.org/10.1007/978-3-642-01932-6_48.

Leven, J., Burschka, D., Kumar, R., Zhang, G., Blumenkranz, S., Dai, X.D., Awad, M., Hager, GD, Marohn, M, Choti, M, Hasser, C, T., R., 2005. DaVinci canvas: a telerobotic surgical system with integrated, robot-assisted, laparoscopic ultrasound capability. Med. Image. Comput. Comput. Assist. Interv. 8, 811–818. https://doi.org/10.1007/11566465_100.

Liang, K., Rogers, Albert J., Light, E.D., Allmen, D.von, 2011. 3D ultrasound guidance of autonomous robotic breast biopsy: feasibility study. Ultrasound Med. Biol. 36, 173–177. https://doi.org/10.1016/j.ultrasmedbio.2009.08.014.3D.

Lin, A.W., Trejos, A.L., Mohan, S., Bassan, H., Kashigar, A., Patel, R.V., Malthaner, R.A., 2008. Electromagnetic navigation improves minimally invasive robot-assisted lung brachytherapy. Comput. Aided Surg. 13, 114–123. https://doi.org/10.3109/10929080801969725.

Liu, Y., Ji, W., Wang, H., Luo, Y., Wang, X., Lv, S., Dong, J., 2015. Robotic spleen-preserving laparoscopic distal pancreatectomy : a single-centered Chinese experience. World J. Surg. Oncol. 13, 1–8. https://doi.org/10.1186/s12957-015-0671-x.

Long, J.A., Hungr, N., Baumann, M., Descotes, J.L., Bolla, M., Giraud, J.Y., Rambeaud, J.J., Troccaz, J., 2012a. Development of a novel robot for transperineal needle based interventions: focal therapy, brachytherapy and prostate biopsies. J. Urol. 188, 1369–1374. https://doi.org/10.1016/j.juro.2012.06.003.

Long, J.A., Lee, B.H., Guillotreau, J., Autorino, R., Laydner, H., Yakoubi, R., Rizkala, E., Stein, R.J., Kaouk, J.H., Haber, G.P., 2012b. Real-time robotic transrectal ultrasound navigation during robotic radical prostatectomy: initial clinical experience. Urology 80, 608–613. https://doi.org/10.1016/j.urology.2012.02.081.

Makuuchi, M., Torzilli, G., Machi, J., 1998. History of intraoperative ultrasound. Ultrasound Med. Biol. 24, 1229–1242. https://doi.org/10.1016/S0301-5629(98)00112-4.

Mallapragada, V., Sarkar, N., Podder, T.K., 2007. A robotic system for real-time tumor manipulation during image guided breast biopsy. In: Proc. 7th IEEE Int. Conf. Bioinforma. Bioeng. BIBE, pp. 204–210. https://doi.org/10.1109/BIBE.2007.4375566.

Mallapragada, V., Sarkar, N., Podder, T.K., 2008. Robotic system for tumor manipulation and ultrasound image guidance during breast biopsy. In: 2008 30th Annu. Int. Conf. IEEE Eng. Med. Biol. Soc., pp. 5589–5592. https://doi.org/10.1109/IEMBS.2008.4650481.

Mallapragada, V.G., Sarkar, N., Podder, T.K., 2009. Robot-assisted real-time tumor manipulation for breast biopsy. IEEE Trans. Robot. 25, 316–324. https://doi.org/10.1109/TRO.2008.2011418.

Matlaga, B.R., Eskew, L.A., McCullough, D.L., 2003. Prostate biopsy: indications and technique. J. Urol. 169, 12–19. https://doi.org/10.1016/S0022-5347(05)64024-4.

Mohareri, O., Ischia, J., Black, P.C., Schneider, C., Lobo, J., Goldenberg, L., Salcudean, S.E., 2014. Intraoperative registered transrectal ultrasound guidance for robot-assisted laparoscopic radical prostatectomy. J. Urol. 193, 1–11. https://doi.org/10.1016/j.juro.2014.05.124.

Moreira, P., Misra, S., 2015. Biomechanics-based curvature estimation for ultrasound-guided flexible needle steering in biological tissues. Ann. Biomed. Eng. 43, 1716–1726. https://doi.org/10.1007/s10439-014-1203-5.

Morse, J., Terrasini, N., Wehbe, M., Philippona, C., Zaouter, C., Cyr, S., Hemmerling, T.M., 2014. Comparison of success rates, learning curves, and inter-subject performance variability of robot-assisted and manual ultrasound-guided nerve block needle guidance in simulation. Br. J. Anaesth. 112, 1092–1097. https://doi.org/10.1093/bja/aet440.

Nadeau, C., Ren, H., Krupa, A., Dupont, P., 2015. Intensity-based visual servoing for instrument and tissue tracking in 3D ultrasound volumes. IEEE Trans. Autom. Sci. Eng. 12, 367–371. https://doi.org/10.1109/TASE.2014.2343652.

Nadler, R.B., Perry, K.T., Smith, N.D., 2009. Hybrid laparoscopic and robotic ultrasound-guided radiofrequency ablation-assisted clampless partial nephrectomy. Urology 74, 202–205. https://doi.org/10.1016/j.urology.2008.08.498.

Nelson, T.R., Nebeker, J., Denton, S., Cervino, L.I., Pretorius, D.H., Boone, J.M., 2007. Performance characterization of a volumetric breast ultrasound scanner. Proc. SPIE 6510, 1605–7422. https://doi.org/10.1117/12.708325.

Nelson, T.R., Tran, A., Fakourfar, H., Nebeker, J., 2012. Positional calibration of an ultrasound image-guided robotic breast biopsy system. J. Ultrasound Med. 31, 351–359 2012.

Neshat, H.R.S., Patel, R.V., 2008. Real-time parametric curved needle segmentation in 3D ultrasound images. In: Proc. 2nd Bienn. IEEE/RAS-EMBS Int. Conf. Biomed. Robot. Biomechatronics, BioRob 2008, pp. 670–675. https://doi.org/10.1109/BIOROB.2008.4762877.

Neubach, Z., Shoham, M., 2010. Ultrasound-guided robot for flexible needle steering. IEEE Trans. Biomed. Eng. 57, 799–805. https://doi.org/10.1109/TBME.2009.2030169.

Newell, M.S., Mahoney, M.C., 2014. Ultrasound-guided percutaneous breast biopsy. Tech. Vasc. Interv. Radiol. 17, 23–31. https://doi.org/10.1053/j.tvir.2013.12.005.

Nguyen, C.T., Jones, J.S., 2011. Focal therapy in the management of localized prostate cancer. BJU Int 107, 1362–1368. https://doi.org/10.1111/j.1464-410X.2010.09975.x.

Noble, J.A., 2010. Ultrasound image segmentation and tissue characterization. Proc. Inst. Mech. Eng. Part H J. Eng. Med. 224, 307–316. https://doi.org/10.1243/09544119JEIM604.

Nota, C.L.M.A., Molenaar, I.Q., van Santvoort, H.C., Borel Rinkes, I.H.M., Hagendoorn, J., 2016. Robot-assisted laparoscopic liver resection: a systematic review of the literature. Hpb. 18 https://doi.org/10.1016/j.hpb.2016.01.146 .

Novotny, P.M., Stoll, J.A., Vasilyev, N.V., del Nido, P.J., Dupont, P.E., Zickler, T.E., Howe, R.D., 2007. GPU based real-time instrument tracking with three-dimensional ultrasound. Med. Image Anal. 11, 458–464. https://doi.org/10.1016/j.media.2007.06.009.

Okazawa, S.H., Ebrahimi, R., Chuang, J., Rohling, R.N., Salcudean, S.E., 2006. Methods for segmenting curved needles in ultrasound images. Med. Image Anal. 10, 330–342. https://doi.org/10.1016/j.media.2006.01.002.

Ophir, J., Alam, S.K., Garra, B., Kallel, F., Konofagou, E., Krouskop, T., Varghese, T., 1999. Elastography: ultrasonic estimation and imaging of the elastic properties of tissues. Proc. Inst. Mech. Eng. H. 213, 203–233. https://doi.org/10.1243/0954411991534933.

Padhani, A.R., Khoo, V.S., Suckling, J., Husband, J.E., Leach, M.O., Dearnaley, D.P., 1999. Evaluating the effect of rectal distension and rectal movement on prostate gland position using cine MRI. Int. J. Radiat. Oncol. Biol. Phys. 44, 525–533. https://doi.org/10.1016/S0360-3016(99)00040-1.

Papalia, R., Simone, G., Ferriero, M., Costantini, M., Guaglianone, S., Forastiere, E., Gallucci, M., 2012. Laparoscopic and robotic partial nephrectomy with controlled hypotensive anesthesia to avoid hilar clamping : feasibility, safety and perioperative functional outcomes. JURO 187, 1190–1194. https://doi.org/10.1016/j.juro.2011.11.100.

Patriti, A., Ceccarelli, G., Bartoli, A., Spaziani, A., Lapalorcia, L.M., Casciola, L., 2009. Laparoscopic and robot-assisted one-stage resection of colorectal cancer with synchronous liver metastases: a pilot study. J. Hepatobiliary. Pancreat. Surg. 16, 450–457. https://doi.org/10.1007/s00534-009-0073-y.

Picard, F., Deep, K., Jenny, J.Y., 2016. Current state of the art in total knee arthroplasty computer navigation. Knee surgery, sport. Traumatol. Arthrosc. 24, 3565–3574. https://doi.org/10.1007/s00167-016-4337-1.

Podder, T.K., Ng, W.S., Yu, Y., 2007. Multi-channel robotic system for prostate brachytherapy. In: Annu. Int. Conf. IEEE Eng. Med. Biol. - Proc., pp. 1233–1236. https://doi.org/10.1109/IEMBS.2007.4352520.

Poulou, L.S., Botsa, E., Thanou, I., Ziakas, P.D., Thanos, L., 2015. Percutaneous microwave ablation vs radiofrequency ablation in the treatment of hepatocellular carcinoma. World J. Hepatol. 7, 1054–1063. https://doi.org/10.4254/wjh.v7.i8.1054.

Preiswerk, F., Toews, M., Cheng, C., Chiou, J.G., Mei, C., Schaefer, L.F., Hoge, W.S., Schwartz, B.M., Panych, L.P., Madore, B., 2016. Hybrid MRI-ultrasound acquisitions, and scannerless real-time imaging. Magn. Reson. Med. 0, 1–12. https://doi.org/10.1002/mrm.26467.

Presti, J.C., 2008. Biopsy strategies-how many and where ? In: Jones, J.S. (Ed.) Prostate Biopsy. Curr. Clin. Urol. Humana Press, pp. 165–178.

Qiu, W., Yuchi, M., Ding, M., Tessier, D., Fenster, A., 2013. Needle segmentation using 3D Hough transform in 3D TRUS guided prostate transperineal therapy. Med. Phys. 40, 42902. https://doi.org/10.1118/1.4795337.

Rao, A.R., Gray, R., Mayer, E., Motiwala, H., Laniado, M., Karim, O., 2013. Occlusion angiography using intraoperative contrast-enhanced ultrasound scan (CEUS): a novel technique demonstrating segmental renal blood supply to assist zero-ischaemia robot-assisted partial nephrectomy. Eur. Urol. 63, 913–919. https://doi.org/10.1016/j.eururo.2012.10.034.

Reddy, K.E., Light, E.D., Rivera, D.J., Kisslo, J.A., Smith, S.W., 2008. Color Doppler imaging of cardiac catheters using vibrating motors. Ultrason. Imaging 28, 247–250.

Reigstad, O., Grimsgaard, C., 2006. Complications in knee arthroscopy. Knee surgery, sport. Traumatol. Arthrosc. 14, 473–477. https://doi.org/10.1007/s00167-005-0694-x.

Ren, H., Anuraj, B., Dupont, P.E., 2017. Varying ultrasound power level to distinguish surgical instruments and tissue. Med. Biol. Eng. Comput. 1–15. https://doi.org/10.1007/s11517-017-1695-x.

Ren, H., Dupont, P.E., 2011. Tubular structure enhancement for surgical instrument detection in 3D ultrasound. In: Proc. Annu. Int. Conf. IEEE Eng. Med. Biol. Soc. EMBS, pp. 7203–7206. https://doi.org/10.1109/IEMBS.2011.6091820.

Ren, H., Vasilyev, N.V, Dupont, P.E., 2011. Detection of curved robots using 3D ultrasound. Rep. U. S. 2011, 2083–2089. https://doi.org/10.1109/IROS.2011.6094915.

Rogers, C.G., Laungani, R., Bhandari, A., Krane, L.S., Eun, D., Patel, M.N., Boris, R., Shrivastava, A., Menon, M., 2009. Maximizing console surgeon independence during robot-assisted renal surgery by using the fourth arm and TilePro. J. Endourol. 23, 115–121. https://doi.org/10.1089/end.2008.0416.

Rohling, R., Gee, A., Berman, L., 1999. A comparison of freehand three-dimensional ultrasound reconstruction techniques. Med. Image Anal. 3, 339–359.

Rusinkiewicz, S., Levoy, M., 2001. Efficient variants of the ICP algorithm. 3-D digit. Imaging Model. IEEE.

Sabo, B., Dodd, G.D., Halff, G.A., Naples, J.J., 1999. Anesthetic considerations in patients undergoing percutaneous radiofrequency interstitial tissue ablation. AANA J 67, 467–468.

Schneider, C., Baghani, A., Rohling, R., Salcudean, S., 2012a. Remote ultrasound palpation for robotic interventions using absolute elastography. Med. Image Comput. Comput. Assist. Interv. 15, 42–49.

Schneider, C., Guerrero, J., Nguan, C., Rohling, R., Salcudean, S., 2011. Intra-operative “pick-up” ultrasound for robot assisted surgery with vessel extraction and registration: a feasibility study. Second International Conference, IPCAI 2011 https://doi.org/10.1007/978-3-642-29066-4{_}11.

Schneider, C.M., Peng, P.D., Taylor, R.H., Dachs, G.W., Hasser, C.J., Dimaio, S.P., Choti, M.A., 2012b. Robot-assisted laparoscopic ultrasonography for hepatic surgery. Surgery 151, 756–762. https://doi.org/10.1016/j.surg.2011.07.040.

Schols, R.M., Bouvy, N.D., Van Dam, R.M., Stassen, L.P.S., 2013. Advanced intraoperative imaging methods for laparoscopic anatomy navigation: an overview. Surg. Endosc. Other Interv. Tech. 27, 1851–1859. https://doi.org/10.1007/s00464-012-2701-x.

Sharma, N.L., Shah, N.C., Neal, D.E., 2009. Robotic-assisted laparoscopic prostatectomy. Br. J. Cancer 101, 1491–1496. https://doi.org/10.1038/sj.bjc.6605341.

Skowronek, J., 2015. Brachytherapy in the treatment of lung cancer - a valuable solution. J. Contemp. Brachytherapy 7, 297–311. https://doi.org/10.5114/jcb.2015.54038.

Sonn, G.A., Margolis, D.J., Marks, L.S., 2014. Target detection: magnetic resonance imaging-ultrasound fusion-guided prostate biopsy. Urol. Oncol. Semin. Orig. Investig 32, 903–911. https://doi.org/10.1016/j.urolonc.2013.08.006.

Stoianovici, D., Kim, C., Schäfer, F., Huang, C.-M., Zuo, Y., Petrisor, D., Han, M., 2014. Endocavity ultrasound probe manipulators Dan. IEEE ASME Trans. Mechatron. 18, 914–921. https://doi.org/10.1109/TMECH.2012.2195325.Endocavity.

Stoll, J., Ren, H., Dupont, P.E., 2012. Passive markers for tracking surgical instruments in real-time 3-D ultrasound imaging. IEEE Trans. Med. Imaging 31, 563–575. https://doi.org/10.1109/TMI.2011.2173586.

Stone, N.N., Roy, J., Hong, S., Lo, Y.-C., Stock, R.G., 2002. Prostate gland motion and deformation caused by needle placement during brachytherapy. Brachytherapy 1, 154–160. https://doi.org/10.1016/S1538-4721(02)00058-2.

Suematsu, Y., Kiaii, B., Bainbridge, D.T., del Nido, P.J., Novick, R.J., 2007. Robotic-assisted closure of atrial septal defect under real-time three-dimensional echo guide: in vitro study. Eur. J. Cardio-thoracic Surg. 32, 573–576. https://doi.org/10.1016/j.ejcts.2007.06.026.

Sumura, M., Shigeno, K., Hyuga, T., Yoneda, T., Shiina, H., Igawa, M., 2007. Initial evaluation of prostate cancer with real-time elastography based on step-section pathologic analysis after radical prostatectomy: a preliminary study. Int. J. Urol. 14, 811–816. https://doi.org/10.1111/j.1442-2042.2007.01829.x.

Swaney, P.J., Burgner, J., Pheiffer, T.S., Rucker, D.C., Gilbert, H.B., Ondrake, J.E., Simpson, A.L., Burdette, E.C., Miga, M.I., Webster III, R.J., 2012. Tracked 3D ultrasound targeting with an active cannula. SPIE Med. Imaging 1–9. https://doi.org/10.1117/12.912021.

Thienphrapa, P., Elhawary, H., Ramachandran, B., Stanton, D., Popovic, A., 2011. Tracking and characterization of fragments in a beating heart using 3D ultrasound for interventional guidance. In: 14th Int. Conf. Med. Image Comput. Comput. Assist. Interv. MICCAI 2011 6891 LNCS, pp. 211–218. https://doi.org/10.1007/978-3-642-23623-5_27.

Thienphrapa, P., Ramachandran, B., Taylor, R.H., Popovic, A., 2012. A system for 3D ultrasound-guided robotic retrieval of foreign bodies from a beating heart. In: 4th IEEE RAS EMBS Int. Conf. Biomed. Robot. Biomechatronics, pp. 743–748. https://doi.org/10.1109/BioRob.2012.6290256.

Trejos, A.L., Lin, A.W., Pytel, M.P., Patel, R.V., Malthaner, R.A., 2007. Robot-assisted minimally invasive lung brachytherapy. Int. J. Med. Robot. Comput. Assist. Surg. MRCAS 3, 41–51. https://doi.org/10.1002/rcs.

Uhečírk, M., Kybic, J., Liebgott, H., Cachard, C., 2010. Model fitting using RANSAC for surgical tool localization in 3-D ultrasound images. IEEE Trans. Biomed. Eng. 57, 1907–1916. https://doi.org/10.1109/TBME.2010.2046416.

Ukimura, O., Desai, M.M., Palmer, S., Valencerina, S., Gross, M., Abreu, A.L., Aron, M., Gill, I.S., 2015. 3-dimensional elastic registration system of prostate biopsy location by real-time 3-dimensional transrectal ultrasound guidance with magnetic resonance/transrectal ultrasound image fusion. J. Urol. 36, 118–125. https://doi.org/10.1016/j.juro.2011.10.124.

Ukimura, O., Nakamoto, M., Gill, I.S., 2012. Three-dimensional reconstruction of renovascular-tumor anatomy to facilitate zero-ischemia partial nephrectomy. Eur. Urol. 61, 211–217. https://doi.org/10.1016/j.eururo.2011.07.068.

Varitimidis, S.E., Venouziou, A.I., Dailiana, Z.H., Christou, D., Dimitroulias, A., 2009. Triple nerve block at the knee for foot and ankle surgery performed by the surgeon : difficulties and efficiency. Foot Ankle Int. 854–859. https://doi.org/10.3113/FAI.2009.0854.

Venkates, S.S., Levenback, B.J., Sehgal, C.M., Sultan, L.R., Bouzghar, G., 2015. Going beyond a first reader: a machine learning methodology for optimizing cost and performance in breast ultrasound diagnosis. Ultrasound Med. Biol. 41, 1–38.

Vernick, W., Atluri, P., 2013. Robotic and minimally invasive cardiac surgery. Anesthesiol. Clin. 31, 299–320. https://doi.org/10.1016/j.anclin.2012.12.002.

Vitiello, V., Lee, S.-L., Cundy, T.P., Yang, G.-Z., 2013. Emerging robotic platforms for minimally invasive surgery. IEEE Rev. Biomed. Eng. 6, 111–126. https://doi.org/10.1177/1938640012445565.

Vrooijink, G.J., Abayazid, M., Misra, S., 2013. Real-time three-dimensional flexible needle tracking using two-dimensional ultrasound. Proc. IEEE Int. Conf. Robot. Autom. 1688–1693. https://doi.org/10.1109/ICRA.2013.6630797.

Walsh, T.M., Borahay, M.A., Fox, K.A., Kilic, G.S., 2013. Robotic-assisted, ultrasound-guided abdominal cerclage during pregnancy: overcoming minimally invasive surgery limitations? J. Minim. Invasive Gynecol. 20, 398–400. https://doi.org/10.1016/j.jmig.2013.01.001.

Wang, Y., Gao, C.qing, Wang, G., Wang, J.li, 2012. Transesophageal echocardiography guided cannulation for peripheral cardiopulmonary bypass during robotic cardiac surgery. Chin. Med. J. (Engl.). 125, 3236–3239. https://doi.org/10.3760/cma.j.issn.0366-6999.2012.18.007.

Wang, Y., Gao, C., Wang, J., Yang, M., 2011. The role of intraoperative transesophageal echocardiography in robotic mitral valve repair. Echocardiography 28, 85–91. https://doi.org/10.1111/j.1540-8175.2010.01274.x.

Wang, Y., Wang, G., Gao, C.Q., 2013. Ultrasound-guided cannulation of the internal jugular vein in robotic cardiac surgery. Chin. Med. J. (Engl.). 126, 2414–2417. https://doi.org/10.3760/cma.j.issn.0366-6999.20123005.

Whitman, J., Fronheiser, M.P., Ivancevich, N.M., Smith, S.W., 2007. Autonomous surgical robotics using 3-D ultrasound guidance: feasibility study. Ultrason. Imaging 29, 213–219. https://doi.org/10.1177/016173460702900402.

Woo, Y., Choi, G.H., Min, B.S., Hyung, W.J., 2014. Novel application of simultaneous multi-image display during complex robotic abdominal procedures. BMC Surg 14, 1–7. https://doi.org/10.1186/1471-2482-14-13.

Wu, L., Song, S., Wu, K., Lim, C.M., Ren, H., 2016. Development of a compact continuum tubular robotic system for nasopharyngeal biopsy. Med. Biol. Eng. Comput. 1–15. https://doi.org/10.1007/s11517-016-1514-9.

Wu, L., Tan, B.L.W., Ren, H., 2015a. Prototype development of a hand-held robotic light pipe for intraocular procedures. 2015 IEEE International Conference on Robotics and Biomimetics (ROBIO) https://doi.org/10.1109/ROBIO.2015.7418795.

Wu, X., Housden, J., Ma, Y., Razavi, B., Rhode, K., Rueckert, D., 2015b. Fast catheter segmentation from echocardiographic sequences based on segmentation from corresponding X-ray fluoroscopy for cardiac catheterization interventions. IEEE Trans. Med. Imaging 34, 861–876. https://doi.org/10.1109/TMI.2014.2360988.

Xu, J., Chen, K., Yang, X., Wu, D., Zhu, S., 2007. Adaptive level set method for segmentation of liver tumors in minimally invasive surgery using ultrasound images. In: 2007 1st Int. Conf. Bioinforma. Biomed. Eng., pp. 1091–1094. https://doi.org/10.1109/ICBBE.2007.282.

Xu, J., Jia, Z.-z., Song, Z.-j., Yang, X.-d., Chen, K., Liang, P., 2010. Three-dimensional ultrasound image-guided robotic system for accurate microwave coagulation of malignant liver tumours. Int. J. Med. Robot. 6, 256–268. https://doi.org/10.1002/rcs.

Xu, S., Kruecker, J., Turkbey, B., Glossop, N., Singh, A.K., Choyke, P., Pinto, P., Wood, B.J., 2008. Real-time MRI-TRUS fusion for guidance of targeted prostate biopsies. Comput. Aided Surg. 13, 255–264. https://doi.org/10.3109/10929080802364645.

Yakoubi, R., Autorino, R., Laydner, H., Guillotreau, J., White, M.A., Hillyer, S., Spana, G., Khanna, R., Isaac, W., Haber, G.-P., Stein, R.J., H., J.K., 2012. Initial laboratory experience with a novel ultrasound probe for standard and single-port robotic kidney surgery: increasing console surgeon autonomy and minimizing instrument clashing. Int. J. Med. Robot. 8, 201–205. https://doi.org/10.1002/rcs.

Yang, L., Wang, J., Kobayashi, E., Ando, T., Yamashita, H., Sakuma, I., Chiba, T., 2014. Image mapping of untracked free-hand endoscopic views to an ultrasound image-constructed 3D placenta model. Int. J. Med. Robot. Comput. Assist. Surg. 11, 223–234. https://doi.org/10.1002/rcs.1592.

Yousef, B., Patel, R., Moallem, M., 2007. An ultrasound probe holder for image-guided robot-assisted prostate brachytherapy. In: Proc. - IEEE Int. Conf. Robot. Autom., pp. 232–237. https://doi.org/10.1109/ROBOT.2007.363792.

Yu, Y., Podder, T.K., Zhang, Y.D., Ng, W.S., Misic, V., Sherman, J., Fuller, D., Rubens, D.J., Strang, J.G., Brasacchio, R.A., Messing, E.M., 2007. Robotic system for prostate brachytherapy. Comput. Aided Surg. 12, 366–370. https://doi.org/10.3109/10929080701746926.

Yuen, S.G., Kettler, D.T., Howe, R.D., 2008. Robotic motion compensation for beating intracardiac surgery. In: 2008 10th Int. Conf. Control. Autom. Robot. Vision, ICARCV 2008, 28, pp. 617–622. https://doi.org/10.1109/ICARCV.2008.4795589.

Zhang, S., Jiang, S., Yang, Z., Liu, R., Yang, Yunpeng, H., L., 2016. An ultrasound image navigation robotic prostate brachytherapy system based on US to MRI deformable image registration method. Hell. J. Nucl. Med. 19, 223–230.

Zheng, G., Nolte, L.P., 2015. Computer-assisted orthopedic surgery: current state and future perspective. Comput. Orthop. Surg. 2 https://doi.org/10.3389/fsurg.2015.00066 .

Zhou, H., Qiu, W., Ding, M., Zhang, S.. Automatic needle segmentation in 3D ultrasound images using 3D improved hough transform - art. no. 691821 Med. Imaging 2008 Vis. Image-Guided Proced. Model. Pts 1 2 6918, 91821. https://doi.org/10.1117/12.770077.

Further readings

Azizian, M., Najmaei, N., Khoshnam, M., Patel, R., 2015. Visual servoing in medical robotics: a survey. Part II: tomographic imaging modalities – techniques and applications. Int. J. Med. Robot. Comput. Assist. Surg. MRCAS 11, 67–79. https://doi.org/10.1002/rcs.

Wakabayashi, G., Cherqui, D., Geller, D.A., 2016. Recommendations for laparoscopic liver resection: a report from the second international consensus conference held in Morioka. Ann. Surg. 261, 619–629. https://doi.org/10.1097/SLA.0000000000001180.

Wein, W., Brunke, S., Khamene, A., Callstrom, M.R., Navab, N., 2008. Automatic CT-ultrasound registration for diagnostic imaging and image-guided intervention. Med. Image Anal. 12, 577–585. https://doi.org/10.1016/j.media.2008.06.006.

Ye, Z., Yang, Z., Zheng, S., Wang, W.. Robot-assisted laparoscopic surgery for abdominal metastatic melanoma mimicking a gastrointestinal stromal tumor: a case report and review of the literature.

Maria Antico received the BEng. in engineering sciences from the University of Rome Tor Vergata, Italy, in 2014 and MEng. in biomechanical engineering from the Technical University of Delft (The Netherlands) in 2016. She is currently a PhD candidate at Queensland University of Technology (Australia). Her research is focused on advanced tissue recognition techniques for fully automated robotic surgery.

Fumio Sasazawa is an orthopaedic surgeon who received his B.S. degree in engineering from the University of Tokio in 1998. He studied medicine at the Shinshu University School of Medicine (Japan) between 1998 and 2004 and was awarded a Ph.D. degree by the Hokkaido University Graduate School of Medicine (Japan) in 2014. He is currently working as a researcher at the Queensland University of Technology (Australia) in the field of ultrasound-guided autonomous surgery robotic applications.

Liao Wu received his B.S. and Ph.D. degrees in Mechanical Engineering from Tsinghua University in 2008 and 2013, respectively. From 2013 to 2015, he worked as a research fellow with the Department of Biomedical Engineering, National University of Singapore. Since 2016, he has been a vice chancellor research fellow with the Australian Centre for Robotic Vision (ACRV), Queensland University of Technology. Dr. Wu's research mainly focuses on Medical Robotics and Industrial Robotics. Particularly, he is interested in Fundamental Theories such as Kinematics, Calibration, and Application of Lie Group Theory in Robotics.

Anjali Jaiprakash received her B.S. degree in biotechnology from the Bangalore University (India) in 2005 and M.S. degree in biotechnology and business from the Queensland University of Technology (Australia) in 2007. In 2014, she received her Ph.D. degree from Queensland University of Technology. Currently, she is working as Advance Queensland Research Fellow in Queensland University of technology (Australia). Her work merges different disciplines such as medicine, engineering and design, to develop medical devices that translate robotic vision into affordable systems that can be used to improve healthcare outcomes. She has experience in the fields of medical robotics, medical devices, orthopaedics.

Jonathan Roberts graduated from the University of Southampton, UK, in 1991 with an Honours degree in Aerospace Systems Engineering. Jonathan furthered his interest in computer vision while completing a PhD (1991–1994) at the University of Southampton where he also developed skills in parallel computing. He is a Professor in Robotics at Queensland University of Technology (QUT), is a Chief Investigator at the Australian Centre for Robotic Vision (ACRV), and is currently QUT's Robotics and Autonomous Systems Discipline Leader. His main research interests are in the areas of Field Robotics, Medical Robotics, Performance Robotics and more recently Design Robotics.

Ross Crawford holds the position of Chair in Orthopaedic Research and Director of the Medical Engineering Research Facility at Queensland University of Technology (Australia). With more than 200 publications, collaborations with Industry and Hospitals, he is an internationally recognized expert in orthopaedics and robotic surgery.

Ajay Pandey is a Vice Chancellor's Senior Research Fellow in Medical and Healthcare Robotics at Queensland University of Technology (Australia). Author of more than 50 research articles, his specialization fields range from advanced materials and renewable energy to cameras and robotic vision.

Davide Fontanarosa is a physicist with a solid background in ultrasound imaging and medical physics. He worked in one of the top institutions for radiation therapy (MAASTRO Clinic, in the Netherlands) and in one of the largest industrial research laboratories in the world, Philips Research, as Senior Scientist. Then he moved to Queensland University of Technology (Brisbane, Australia) to take up a position as Senior Lecturer where he is currently doing research in several fields related to ultrasound and radiation therapy and coordinating two honours courses.